The Analysis of Irregular Flat Plates with Surface Oriented Moment Distribution

By Kolbjorn Saether

Abstract

A general flat slab analysis is presented based on an enhancement to a previously developed methodology referred to as the Structural Membrane Approach (SMA) Saether (1961). This analysis assumes that the slab deforms in such a fashion as to generate a moment field that can be described by a connected region of three basic 3-D moment functions. These moment functions are referred to as Structural Membrane shapes and are similar to the displacement patterns of a stretched elastic membrane subjected to lateral loads. The original formulation of SMA dealt with the calculation of fixed-end moments. The present work extends the capabilities of SMA by enforcing appropriate boundary conditions along their interior and exterior edges through the application of a surface oriented moment distribution. By using this approach for analyzing regular and irregular slab layouts an extremely intuitive and useful methodology results.

Introduction

The present paper deals with the determination of the final bending moments in randomly supported flat plates using the Structural Membrane Approach developed by Saether.(1999). This approach was developed based upon the dualism between the elastic membrane deflection and the plate bending moments as explored in detail by Dr.-Ing. H. Markus in his textbook “Die Theorie elastischer Gewebe und ihre Anwendung auf die Berechnung biegsamer Platten.” (1924). Whereas these analyses dealt with the solution of plate and shell problems with line supported edges, the SMA has extended the analysis to include point-supported structures.

The SMA approach has been compared by Baskaran (2004) to methods such as the ACI-318 Equivalent Frame, the Finite Element Method, the Yield-Line Approach, various Strip Methods and the Triangle Slab Element Approach. In all cases the SMA proved great advantages over existing analytical and numerical approaches. It would deliver results such as peak and average moments at columns, complete moments throughout the slab and accurate column reactions and bending moments for distributed and concentrated loads. Even though the Strip Method by Hillerborg (1996) shares some similarity with SMA in that the slab is analyzed as a network of column and middle strips and can handle regular and irregular slabs, the Strip Method is based on determining “hog” and “soft” lines throughout the slab for which there are no general rules and which results in a complicated analysis. In contrast, SMA is based on a firm, geometric decomposition of the slab into local regions that exactly demarcates the span lengths and widths of the equivalent column and middle strip. Finite element methods offer complete versatility in the analysis of structures but, even in commercial finite element codes specialized for the structural engineering field such as Etabs (2005), there are several difficulties affecting the numerical approach.

Besides the time required to define a structural model; they entail the possibility of introducing modeling errors; a possible lack of convergence of the solution; and some time difficulties in reduction and interpretation of output data.

The SMA offers a straightforward definition of sub-regions within the slab and directly yields the important average column moments required for the design. The advantage that SMA has over finite element approaches is partly because of the fact that the shape of the moment surfaces is determined a priori for the entire field. This is based on an established spatial combination of fundamental solutions for each specific area of the complete layout which is totally described by a limited number of parameters. In finite element analyses, solutions are obtained by discretizing the slab into a field of finite elements and applying appropriate boundary conditions to obtain a numerical solution. The result depends on the solution of a huge system of algebraic equations that only slowly converge to the shape of the moment curves in any given area, making mesh refinement an important consideration. In addition, finite element solutions require significant finess in interpreting the results.

For engineering design, it is generally accepted that peak moments about columns may be reduced to average values due to the cracking of the concrete and yielding of the steel around these supports. While finite element solutions must be laboriously post-processed to obtain average column moments, SMA directly assumes that the column moments are averaged over effective cross-sections assumed for each column. This listing of the average moments, based on the equilibration of fracture mechanisms, is not easily obtained from finite element solutions and is not a standard output of finite element-based structural engineering codes. When implemented in a computer code, the SMA analysis is accomplished with a small numerical effort that is a fraction of what is needed using general finite element method. In addition, SMA is shown to be sufficiently accurate within the 'error-bands' that exist when translating an idealized engineered design to the actual constructed structure. Overall, the SMA method is found to be versatile, fast, accurate and superior to most other analytical approaches (Baskaran, 2004).

SMA utilizes shape functions of local moment fields that are assumed over slab sub domains. These moment functions are obtained from solutions to the governing equations of standard plate theory, in particular the equation expressing the dualism between the elastic membrane deflection and plate bending moments. The 4^{th}-order Kirchhoff governing differential equation for plate deflection is given by

$$\frac{\partial^4 w}{\partial^4 x} + 2\frac{\partial^4 w}{\partial^2 x \partial^2 y} + \frac{\partial^4 w}{\partial^4 y} = \frac{q}{D} \qquad (1)$$

where q is the applied loading, w is the plate displacement, and D is the plate stiffness.

A simple decomposition of Equation (1) using classical moment-deflection relationships leads to two membrane-type 2^{nd}-order equations that describe the moment and displacement fields given by:

$$\frac{\partial^2 M}{\partial^2 x} + \frac{\partial^2 M}{\partial^2 y} = -q \quad (2)$$

$$\frac{\partial^2 w}{\partial^2 x} + \frac{\partial^2 w}{\partial^2 y} = -\frac{M}{D} \quad (3)$$

where M is a combined moment defined by:

$$M = (M_x + M_y)/(1 + v) \quad (4)$$

Both equations have the form of the membrane equation which describes the deflection of a stretched elastic membrane under uniform lateral loading. Equation (3) expresses the relationship between moments and deflection and is not used in the SMA, only solutions to Equation (2) are used to relate moments to applied loads. The simplest solution to the membrane equations consists of Hyperbolic Paraboloids (HP), Elliptical Domes (ED) and Logarithmic Funnels (LF).

The moments M in Equation 4 remains indeterminate as long as the division of q into q_x and q_y components remains an unknown. In dealing with the three basic element shapes in the SMA, the elliptical generality of the basic SMA shapes are assumed circular, thus, application of the ED, the HPs, and the LF are mapped to the distributed slab by a series of observations.

The circular, parabolic dome (CD), if subjected to a lateral uniformly distributed load and a constant horizontal thrust along all four edges, because of its symmetry around its center and its symmetry around any two orthogonal horizontal lines must divide the load q in a 50/50 split qx = qy.

The square HP with its positively curved strips in one direction an negatively curved strips in the orthogonal direction can carry the load q only in the positively curved direction. In the other direction a down ward load develops that serves to add to the load that the first direction must carry.

If this unit has its negatively strips abut the dome edges, for equilibrium reasons the thrust in these ribs H1hp must equal the thrust Hd in the dome unit with the result that those ribs cause a downward reaction of –q/2. The positively curved roibs must consequently carry the total load plus this component q/2. The thrust at the base of this unit is therefore H2hp = 3 Hd with an upward reaction of 3/2q.

The funnel, in order to match the lower edges of the HP in location and slope must consist of triangular slivers of inverted domes. The thrust in these negatively curved strips, in order to maintain equilibrium with the HP must be of the magnitude of HP2 = 3Hd. The result is a downward uniform load of 6q uniformly distributed over these surfaces. The only way to support this is that these units develop radially oriented ribs with horizontal radial thrusts with increasing intensity as they extend toward the center of the unit of sufficient magnitude to balance the total downward load equal 7q.

The normal to the radially oriented strips make up horizontal rings. These rings are capable of developing ring tensions to increase the horizontal thrusts in the redial rings without disturbing the overall equilibrium of the unit. The detailed calculation of the thrust is complex. By expressing the equilibrium along the upper edges and the lower edges of these inverted domes the following results are obtained, however:

H2f = 1.36 H2hp.

It is generally acknowledged that the membrane carries its load by the tensile force located in the deformed shape of the membrane surface. With the deflection made small enough not to drastically change the uniform stress pattern initially introduced into the membrane, the determination and design of elastic membrane structures is completed simply by measuring the deflections of scale models This very fact has been exploited by Hans Isler of Switzerland (1995) in the construction of several hundred thin shell concrete roof structures, where the shape of these shells were determined by the careful measuring of membrane models of the layouts.

In other words, a dualism exists between the bending moments in flat plates and the deflections of an elastic membrane with the deformed, elastic model picturing the bending moments in a plate supporting a uniformly distributed surface load. In the study of plates and shells by Timoshenko (1959), several references are made to this dualisms. In particular, symmetrical, uniformly loaded, rectangular flat plates and circular, point supported plates are analyzed. Similarly, this elastically deformed membranes, when subjected to different amounts of tension in the two major directions will cause a hyperbolic praboloidal shape to be developed. All of these shapes, the ED, the HP and the LF are governed by a simple set of differential equations with the most elementary expressions describing their bending moments.

Exploiting the simplicity among complex thin-shell analyses, the first premise in the development of the SMA was made. From a series of experiments using uniformly stressed and laterally loaded elastic membranes, with a layout made to simulate a column supported shell with the column arranged in a square pattern, the resulting deformed elastic membrane showed clear indications of containing a composite three basic shells, the dome, the HP and the funnel.

The second premise in the SMA development was reached when realizing that it was possible to determine the boarders between these shapes and determine their individual

geometry required to make the resulting shape continuous and match the original elastically deformed shape.

It was shown by Saether (1961) that these shapes can combine into a continuous surface carrying a uniform load on this membrane from one column support to the next column with uniform horizontal thrusts throughout the surface.

The shape of the thin shell and the moments in the flat plate have been determined for column layouts containing square grids as well as equal lateral triangular and hexagonal grids. A rigid algorithm for determining these shapes giving the location of the juncture lines of these shapes to establish the continuity between these shapes has been developed. For these regular shapes the contour lines prove to be circular or hyperbolic.

A small modification in the elastic membrane shape, with only a minor effect on the corresponding moments will allow non-symmetrical layouts to change from elliptical moment contour lines to circular lines and thereby be analyzed with the same ease as the symmetrical shapes.

Through the similarity with the elastic membrane it was in other words possible to describe the bending moments in any plate as a combination of these simple deformed shapes. In their general form, the shapes were unsymmetrical, containing expressions for M_{xy} and M_{yx} . By a slight modification of the shapes, however, it was possible to approximate these by their symmetrical counterparts: the circular dome, the symmetrical HP and the circular funnel.

In the SMA development it has been stipulated that close to any shape can be approximated by a combination of three basic shapes: the Dome: the Hyperbolic Paraboloid and the Funnel. With the analogy between the elastic membrane and the structural membrane counterpart, simple expressions have been developed. When further approximated with symmetrical shapes within each part area further simplifications resulted.

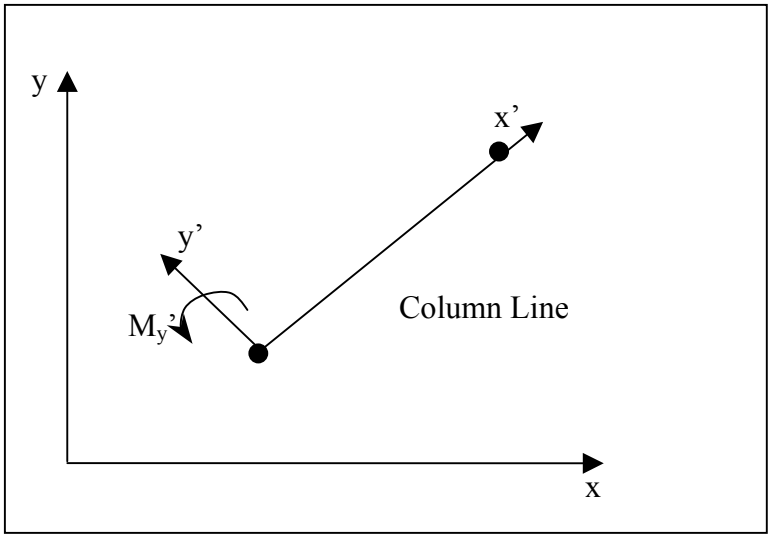

To recap: local regions are determined within the slab through a systematic procedure of discretizing the slab layout in which specific moment functions are assumed. The procedure for determining local moment distribution is an essential aspect of SMA and will be described in following discussions. Within each region of the slab, local coordinates, (x', y'), are defined with the *x*' axis running along lines connecting adjacent columns and the *y*' axis is assumed perpendicular in a counterclockwise sense. (Figure 1). The uniform load *q* is assumed to be equally divided in the orthogonal local directions *x'* and *y'*.

Local field moments in SMA are computed for both x' and y' axis. In the local coordinate system, only principal moments exist such that Equation (2) can be treated as a scalar equation with the moment *M* given by

$$M = H*e$$

Where H is the horizontal thrust and e is the height of the funnel surface at any one location. These shapes are directly used in SMA to compute specific values of the field moments in the local coordinate system.

The flexibility of this approach permits the analysis of randomly supported slab systems. Appropriate boundary conditions are enforced along their interior and exterior edges by the application of a surface oriented moment distribution. At the completion of the analysis, all local moments are transformed into the global coordinate system and summed up to give measures of M_x and M_y throughout the entire slab region.

The fundamental moment functions used in SMA consist of a Logarithmic Funnel (LF), an Elliptical Dome (ED) and a Hyperbolic Paraboloid (HP) as shown in Figure 2. While satisfying the continuity conditions between these fields and maintaining equilibrium within the units and with the external loads, the fields yield accurate values for the fixed-end-moments and the corresponding column reactions for the slab. The arrived at fixed-end-moments are subsequently subjected to a surface oriented moment balancing in which moments are distributed as a function of relative stiffness within the slab and between the slab and the supporting columns. After a solution to the global field moments is determined over the entire slab, individual column loads and moments are modified to account for the final moments assuming a fully elastic system.

In addition, compared to most numerical methods, SMA permits moments as well as column contributory areas and column reactions of irregularly supported slabs to be rapidly evaluated.

Because of the increasing use of finite element methods, it will be emphasized in this paper that SMA yields comparable results to detailed finite element analysis. This demonstration will additionally show the enormous simplification of moment predictions due to the a priori representation of assumed field solutions compared to standard finite element solutions that are based on slowly convergent minimum energy principles. The overall capability of SMA will be shown to result in an ideal theoretical basis for a rapid and versatile design tool.

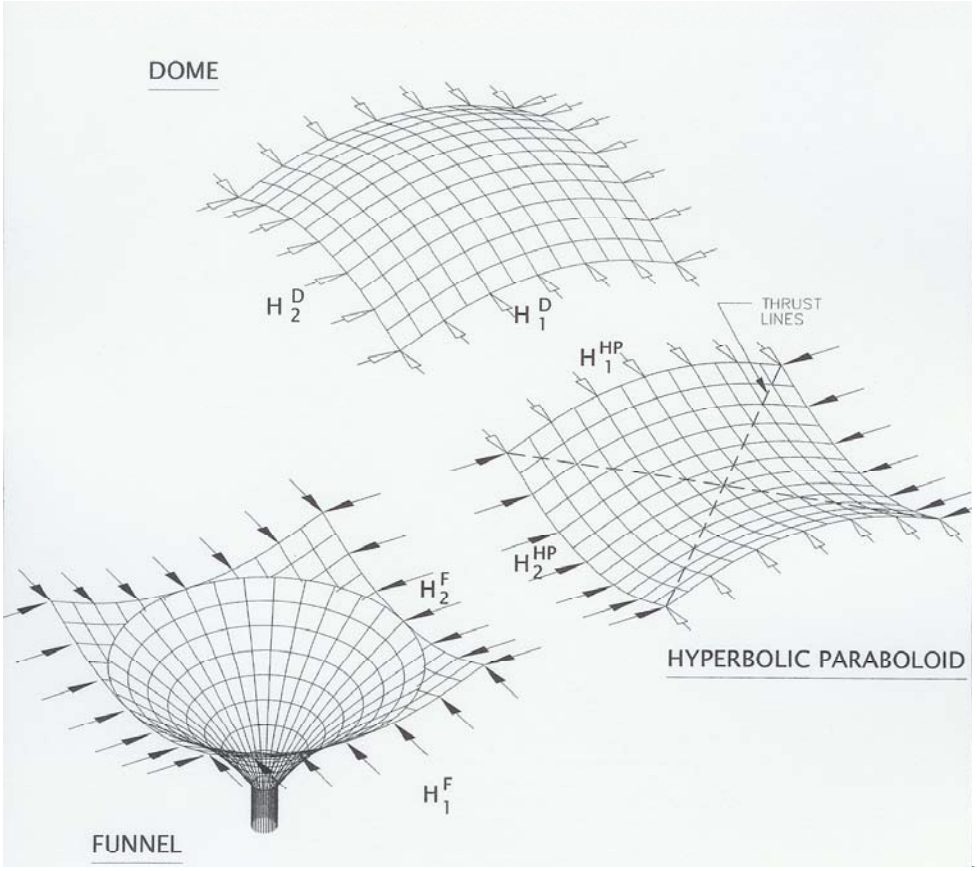

Figure 2. Basic structural membrane units.

SMA Analysis

The first step in the SMA analysis procedures is to establish the specific outline of the geometric regions over which different functional forms of field moments are assumed. Based on a prior understanding of how these moment fields originate, the outline of these regions are determined by identifying geometric quantities referred to as "column-lines" and "thrust-lines". The geometry of the resulting regions are further defined by quantities known as "fall-lines". As detailed in Saether 1961, circular LF moment fields are assumed centered over each column locations, ED fields are assumed interior to local regions bounded by column lines, and HP moment fields are defined centered across sections of column lines such that LF and ED fields are seamlessly connected. Details of the construction of these geometric quantities are outlined below.

Column lines in the SMA are the dominating sets of lines connecting adjacent columns that define interior span lengths. These are readily identified for rectangular (Figure 3),

equilateral triangular (Figure 4) and equal-sided hexagonal layouts (Figure 5). For randomly oriented columns, the definition of column lines requires some additional guidance (Figure 12). In all cases, column lines exist between adjacent exterior columns. For interior columns in an irregular layout, a specific set of rules is required to determine the connecting column-lines (Figure 10).

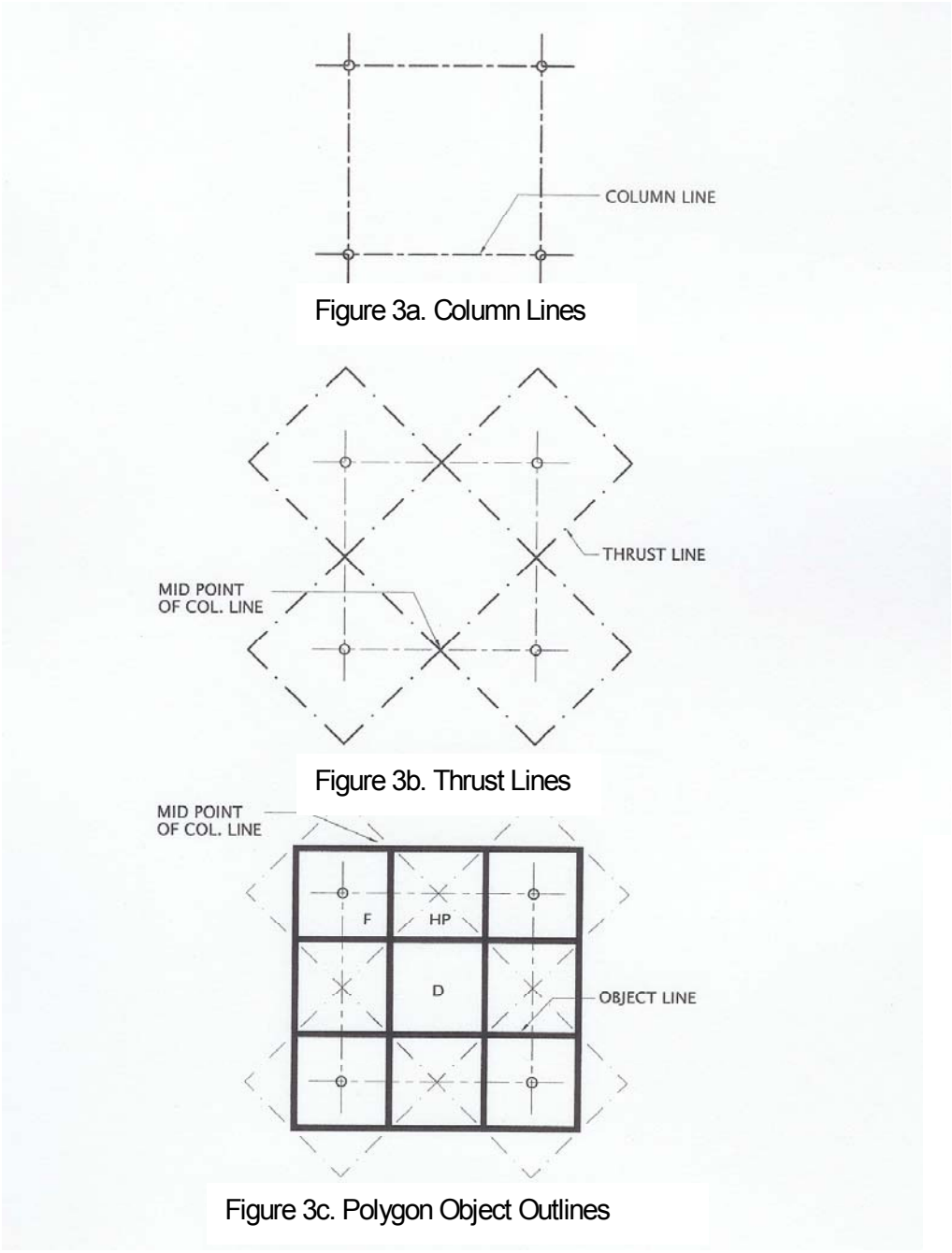

Figure 3. Geometry of square structural membrane layout.

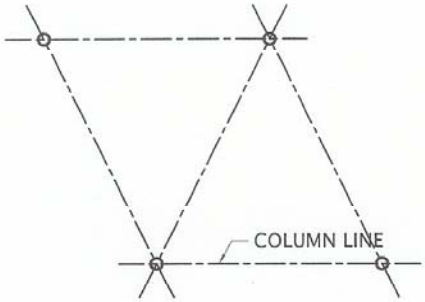

Figure 4a. Column Lines

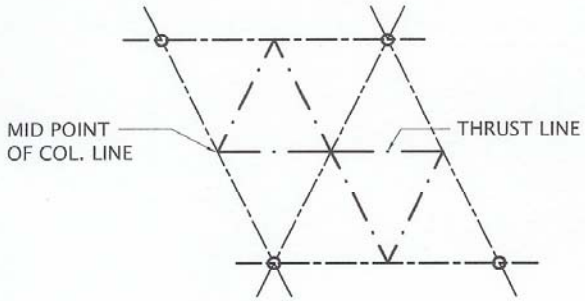

Figure 4. Thrust Lines

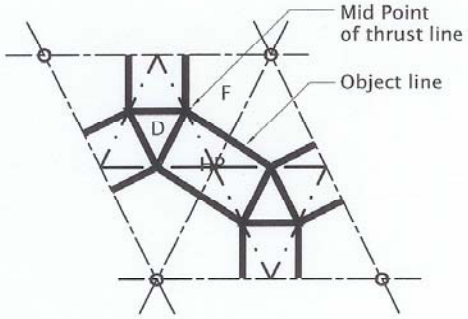

Figure 4c. Object Lines

Figure 4. Geometry of triangular structural membrane layout.

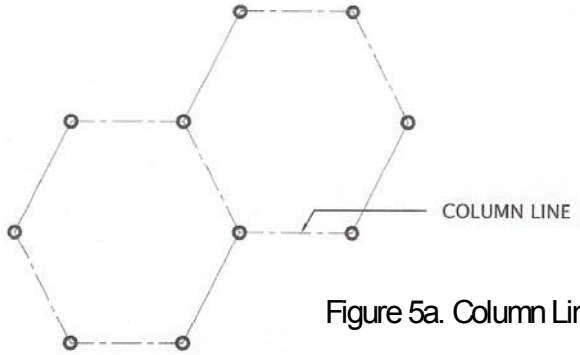

Figure 5a. Column Lines

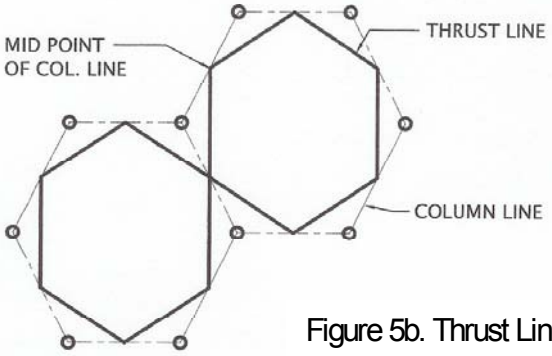

Figure 5b. Thrust Lines

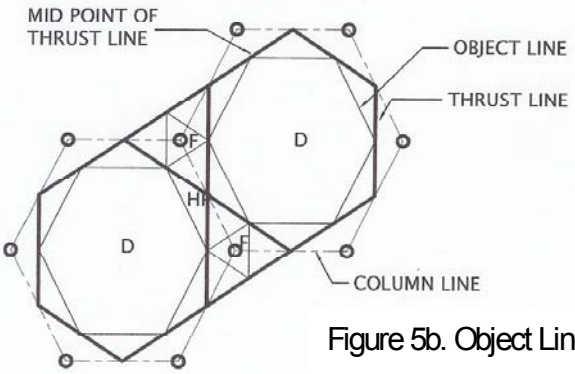

Figure 5b. Object Lines

Figure 5. Geometry of hexagonal structural membrane layout.

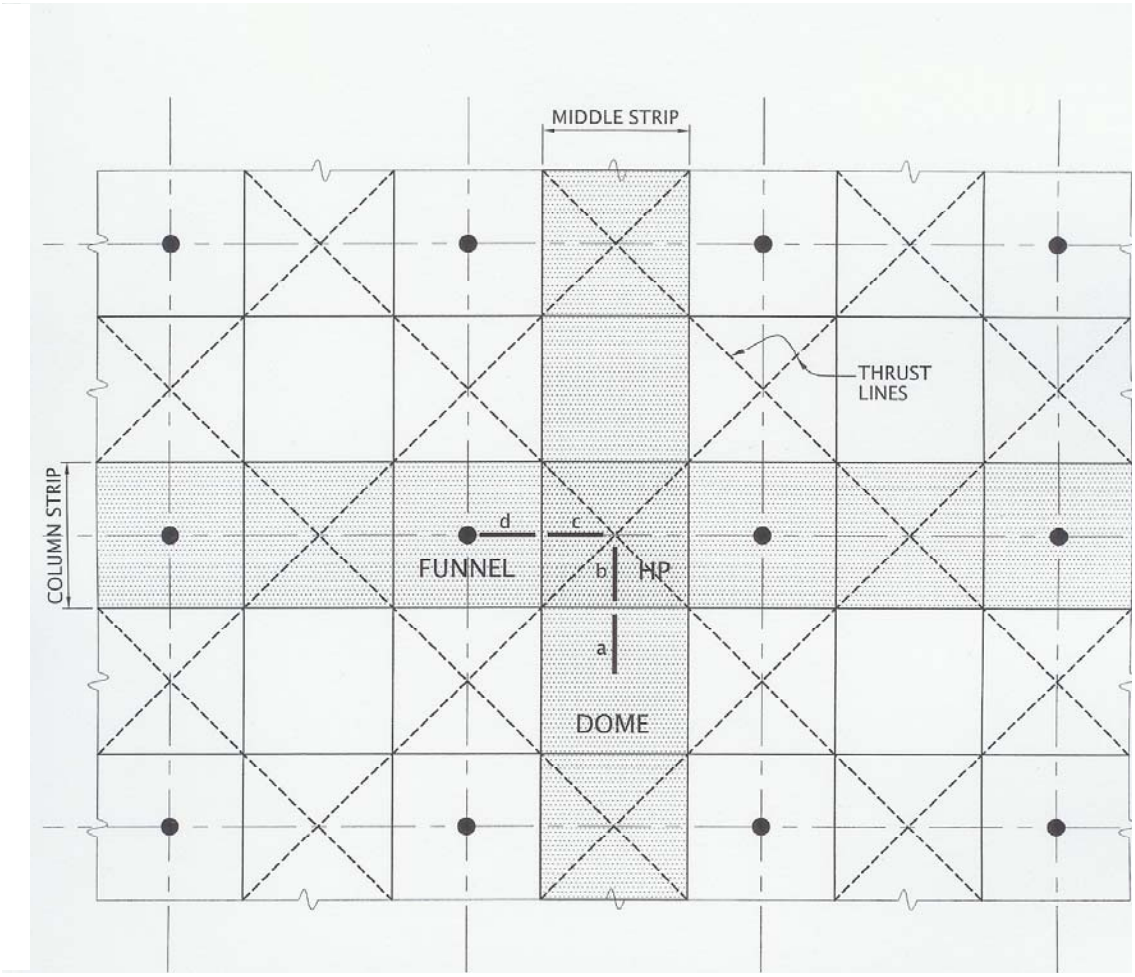

Figure 6. Structural membrane configuration generated for a square-column plan.

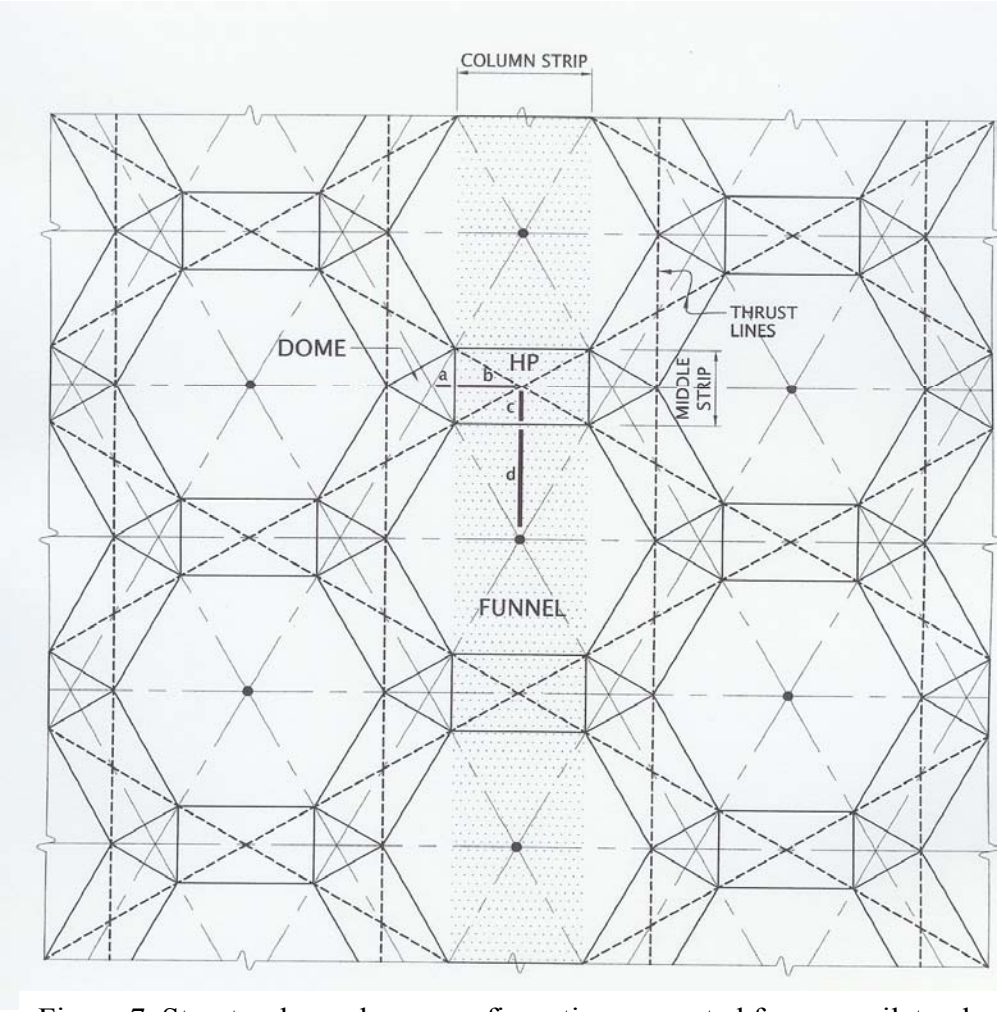

Figure 7. Structural membrane configuration generated for an equilateral-triangular column plan.

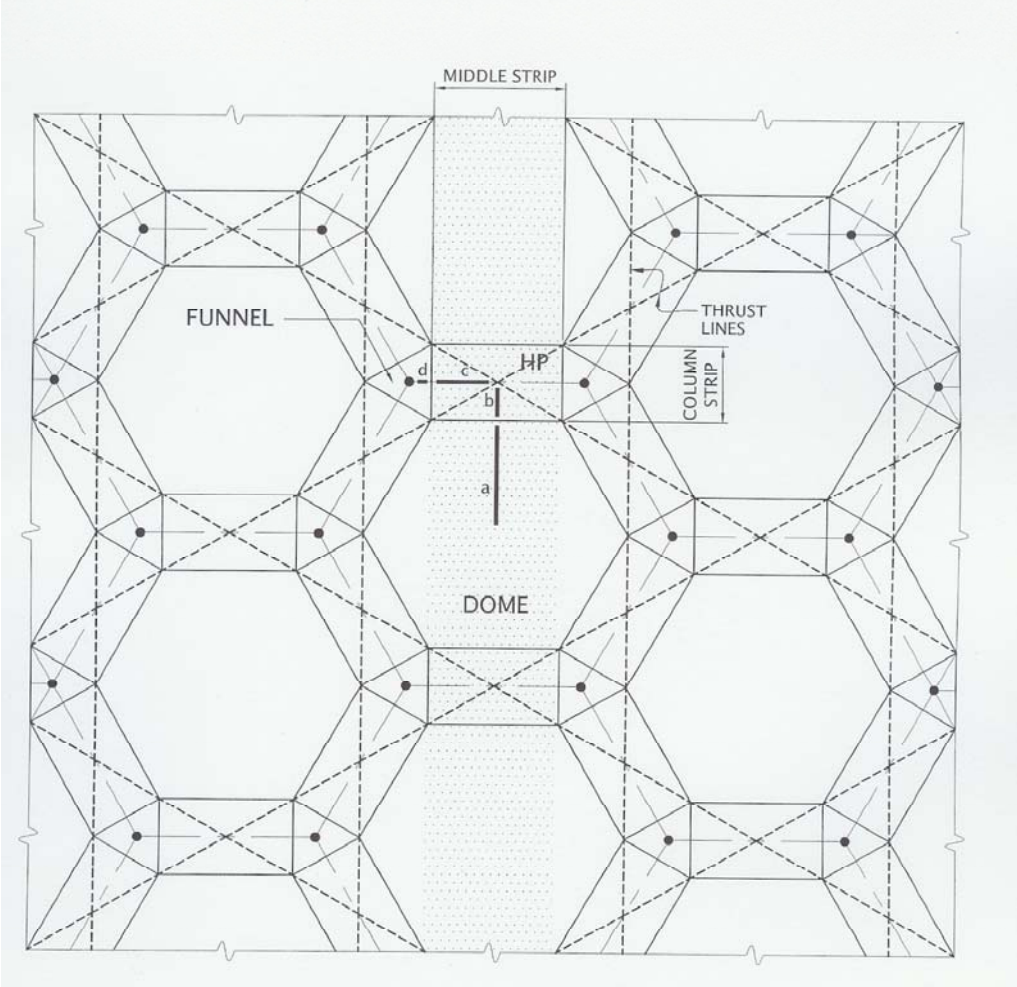

Figure 8. Structural membrane configuration generated for a hexagonal column plan.

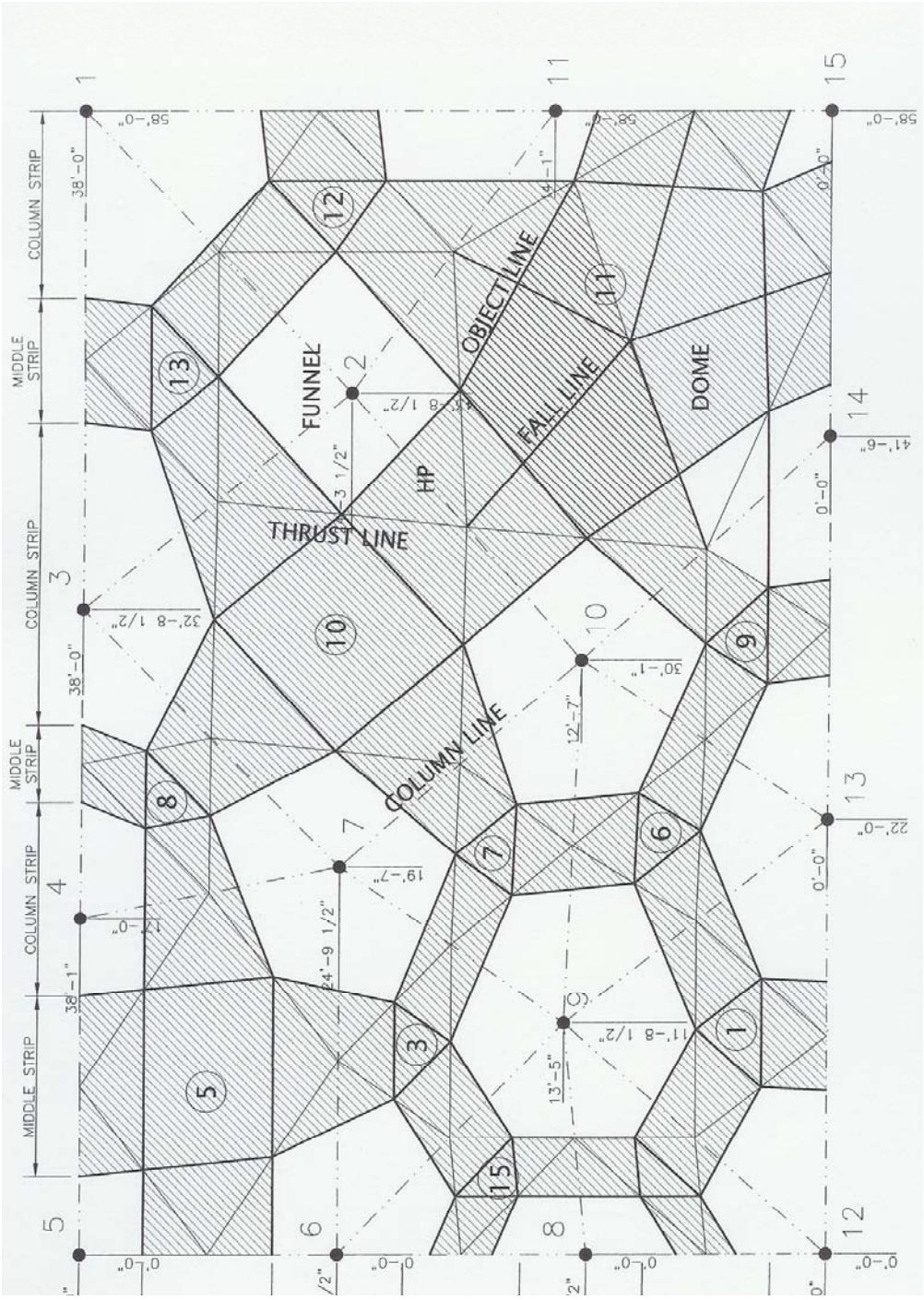

Figure 9. Typical floor plan of an irregular column layout.

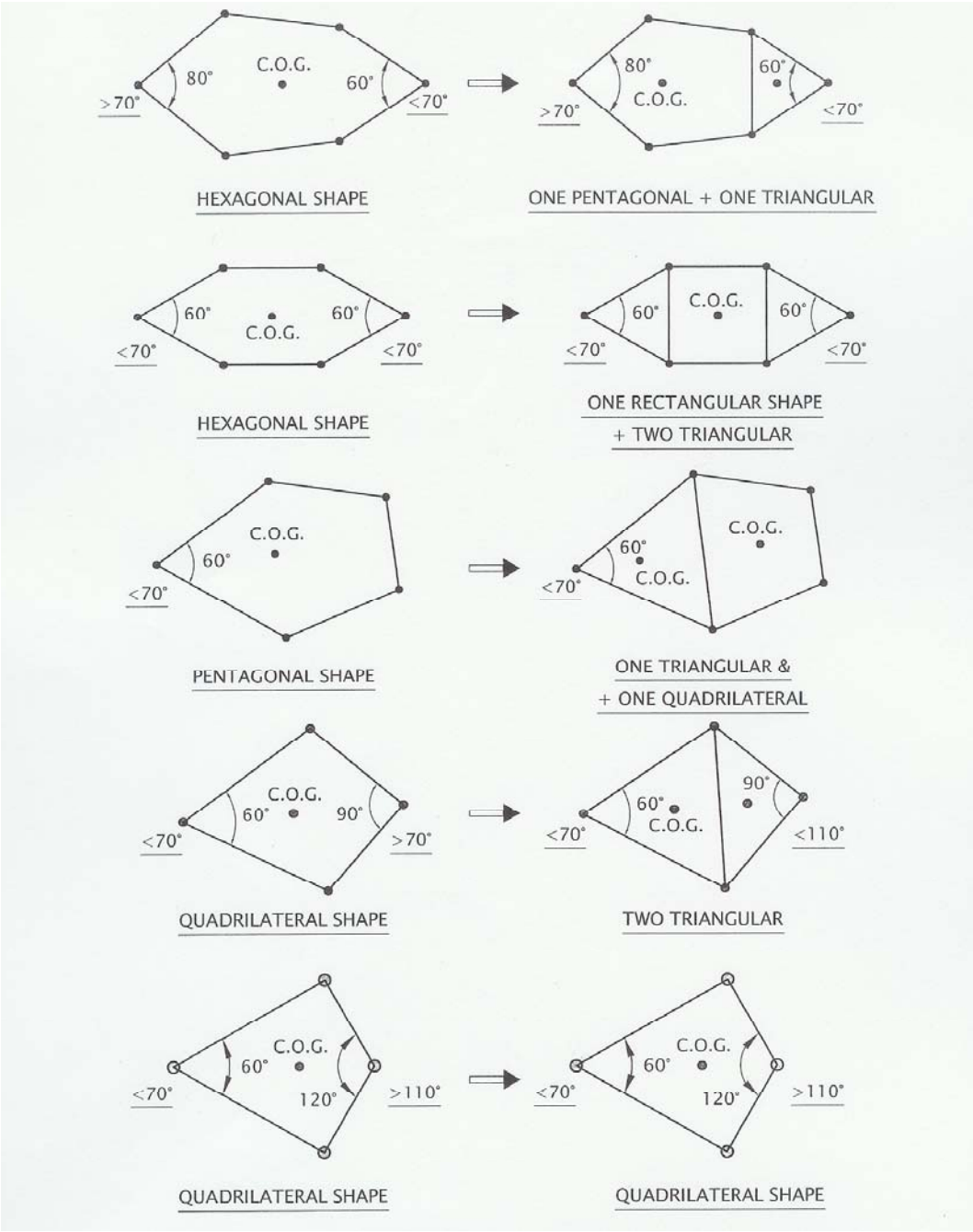

Figure 10. Determination of column lines and basic fields.

The procedure outlined for designating regions in which particular Structural Membrane solutions are assumed involves certain limiting factors. In developing regions based on the initial outline of column lines, several numerical constraints have been identified by the author based on numerical computations. These constraints involve the angles between adjacent column lines and are related to the elastic energy and assumed distribution of Structural Membrane moment shape functions. The following guidelines in discretizing slab regions have been developed to minimize the energy of deformation and, hence, the magnitude of moment distributions over these regions. (Figure 10).

If the angle between two adjacent potential column-lines in the floor plan layout is less than 70°, a column-line will exist between the ends of these two lines, unless, in the case of quadrilateral areas, the opposite angle is larger than 110^{o}. If the initial angle is larger than 70°, no column-line appears between the ends. The angles of 70° and 110° represent the approximate border between two SMA approximations, one using one base area, the other using two areas as explained in the following.

Thrust lines connect the mid-points of any two adjacent column lines (Figure 9). In the thin-shell analogy, these are straight lines that exist within the (HP) and identify the locations of the thrust required to maintain the equilibrium of the shell surface.

The moment field outlines are determined as lines that connect the midpoints of any two adjacent thrust lines. (Figure 9). These lines identify the outlines of the basic units of the moment fields. These are described by the ”fall-line” parameters *a*, *b*, *c* and *d* (Figure 11). These parameters are fundamental to the SMA and are used to calculate the bending moments and column reactions in the slab and supporting columns.

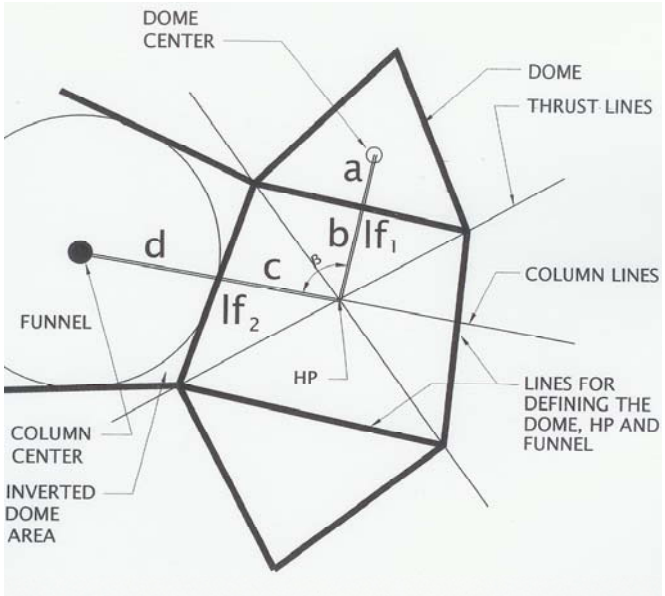

Figure 11. Structural membrane components.

The fall-lines have the following values: $Lf_1 = a + b$ and $Lf_2 = c + d$ as shown in Figure 11. They describe two lines, one Lf_1, extending from the center of the dome to the intersection of the thrust-lines, Lf_2 within the hyperbolic paraboloid. The latter Lf_2 extends from that point to the center of the two supporting columns. These lines Lf_1 and Lf_2 will intersect at an angle β. For all regular layouts (rectangular, equal lateral triangular and hexagonal layouts), the angle β is equal to 90°. For irregular column arrangements, however, this angle may vary from 90°. For these non-orthogonal fall lines the SMA equations would be dealing with non-circular contour lines. To circumvent this, as a first approximation, the component Lf_1 is rotated around its intersection with the Lf_2 lines until β becomes 90^o as shown in Figure 12. At the same time the components *a* and *b* of Lf_1 are multiplied by the factor cos (β - 90^o) to become a_1 and b_1. The effect of this is that the total area defined by the height of the triangle Lf_1 and the base of Lf_2 remains unchanged, but the elliptical components used in the SMA convert to the much more convenient circular outlines.

By using the values 70° and 110° in establishing the controlling column lines, an optimum in accuracy is achieved when using the circular approximation for the moment area outlines. The true transition from unsymmetrical shape to the next would otherwise consist of elliptical or dumb-bell shaped moment-area outlines, with the consequence that their derivations would be beyond simple descriptions. When guided by the limiting angles of 70° and 110° for determining the controlling column-lines, the moment areas are only slightly distorted with the moments changed in the direction of conservative values.

The resulting geometries have been shown in Figures 3 through 5. The slab is divided into regions where each assumes one of the three moment-field functions. Figures 6 through 8 show these developed for symmetrical square, triangular and hexagonal layouts. These are regions over which the different moments are calculated as a first order approximation. The magnitude of these moments depends on the uniform load, the shapes of the regions and the relative location of the supporting columns. With this approach, moment fields may be calculated for both regular and irregular layouts (Figure 9).

There is a similarity in the development of these to the "column-strip" and "middle-strip" assumptions in the ACI-318 Equivalent Frame Method. This is particularly evident in a square layout, which has been shown in Figure 6. It should be noted, however, that in the SMA these shapes provide a more accurate definition of the bending moments as compared to the terms "column-strip moments" and "middle-strip moments" as specified in the Equivalent Frame Design of the code.

The similarity can be summed up as follows: The Elliptical Dome (ED) describes the moments within two intersecting middle strips. The Logarithmic Funnel (LF) represents the moment in two intersecting column-strips and correctly introduces the peak moments at the columns. The Hyperbolic Paraboloid (HP) properly describes the moment distribution at the intersection of middle strips and column strips as these units form the asymmetrical (3-D) moment field typical for the transition between domes and funnels. The interaction between these areas has been shown in Figure 13.

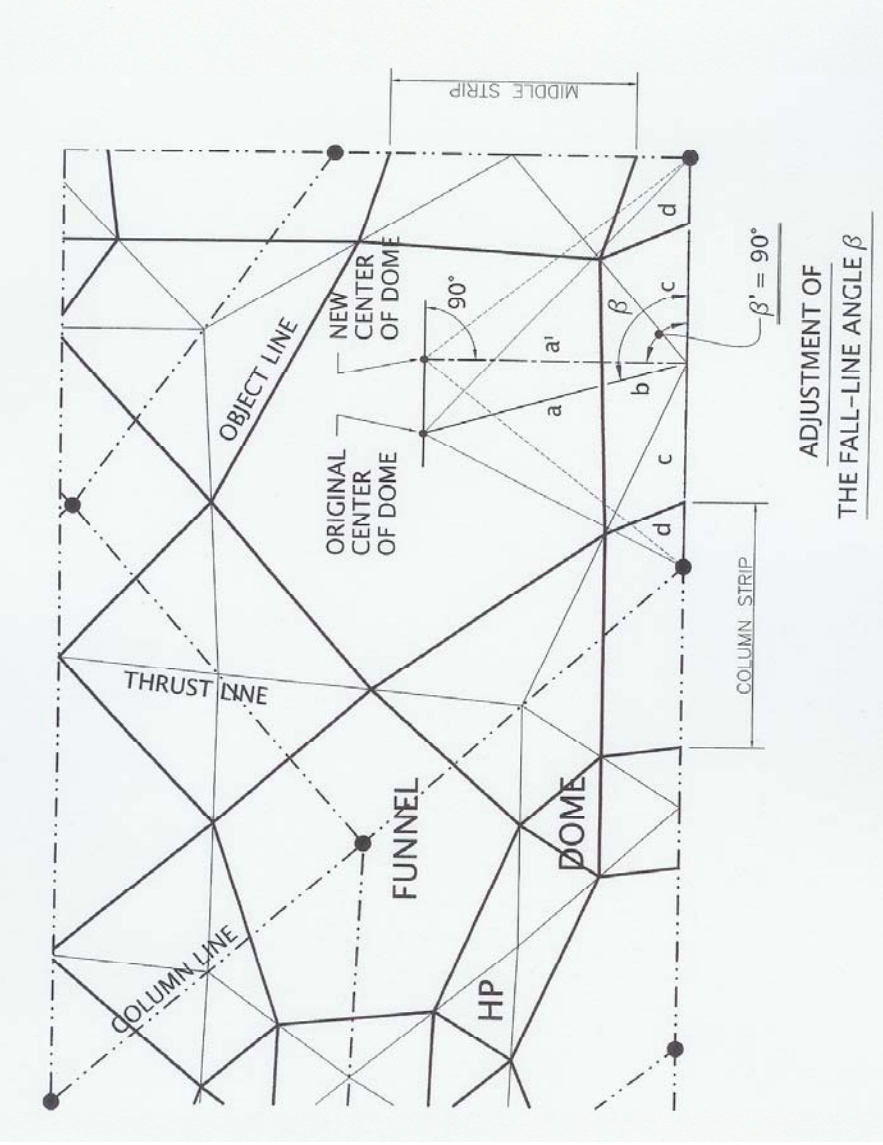

Figure 12. Division into moment fields.

Figure 13. Middle-strip/column-strip interaction.

Once the moment fields have been identified, the entire design is obtained by the following general equations (Saether 995). These equations satisfy all equilibrium and continuity requirements in the SM units. The superscripts D, F and HP refer to domes, funnels and hyperbolic paraboloids, respectively. The geometry of the SM basic element (SMBE) as defined in Figure 9, by the variables *a*, *b*, *c* and *d* is calculated by the following expressions.

The span from one column along the valley HP to the next column is:

$$\mathrm{L}^{\mathrm{HP/F}} = (\mathrm{c}_1 + \mathrm{d}_1) + (\mathrm{c}_2 + \mathrm{d}_2) \tag{4}$$

where $c_1 + d_1$ is the distance from center of HP to center of one column and $c_2 + d_2$ is the distance from the same HP center to the center of the other column as shown in Figure 13.

In arriving at these expressions, full use is made of the analogy between the structural membrane shape equal to the elastic membrane shape, and the bending moments in the corresponding flat plate. The span between the center of one valley HP across the dome to the adjacent valley HP is:

$$L^{D/HP} = (a_1 + b_1) + (a_2 + b_2) \tag{5}$$

Where a_1 and b_1 extend from the center of the dome to the center of the supporting HP; and $a_2 + b_2$ extend from the same dome to the center of the opposite HP. This is shown in Figure 13. For symmetrical layouts these spans are:

$$L^{D/HP} = 2(a + b) \tag{6}$$

$$L^{HP/F} = 2(c + d) \tag{7}$$

To start a layout of SM shells, the dome height h^D is any arbitrary value different from zero selected by the engineer. The ratio of a/b is referred to as $n^{D/HP}$. From the continuity requirements, the ratio of the dome height h^D to the depth of the hyperbolic paraboloid h^{HP} is found to be equal to the same $n^{D/HP}$:

$$\frac{h^D}{h^{HP}} = \frac{a}{b} = n^{D/HP} \tag{8}$$

From the equilibrium requirements and by assuming that for any circular dome the exterior load *q* is divided equally in any two orthogonal directions, the following formulas are derived:

The thrust $H^{D}{}_{1}$ in the dome is:

$$\mathrm{H_1^D} = \frac{\mathrm{qa}^2}{4\mathrm{h^D}} \tag{9}$$

The depth of the hyperbolic paraboloid h^{HP} is calculated as:

$$h^{HP} = \frac{h^{D}}{n^{D/HP}} \tag{10}$$

From the equilibrium requirements it is found that the thrust across the HP must be:

$$H_1^{HP} = H_1^{D} \tag{11}$$

This thrust generates a downward reaction $\mathrm{q_1^{HP}}$ within the HP of the magnitude:

$$\mathrm{q_1^{HP}} = \frac{\mathrm{H_1^{HP}} \cdot \mathrm{h^D} \cdot 2}{(\mathrm{b})^2 \mathrm{n^{D/HP}}} = \frac{2\mathrm{H_1^{HP}h^{HP}}}{\mathrm{b}^2} \tag{12}$$

The orthogonal thrust $H_2{}^{HP}$ in the HP, which is the same as the thrust $H_1{}^{F}$ along the upper rim of the funnel unit along the top of the inverted domes (The complete continuity of the surface is generated by the introduction of four parts of one compatible inverted dome), must carry this load in addition to the given uniform load *w* and is expressed as:

$$\mathrm{H_2^{HP}} = \mathrm{H_1^F} = \frac{(\mathrm{q_1^{HP}} + \mathrm{q}) \cdot (\mathrm{c})^2}{2\mathrm{h^{HP}}} \tag{13}$$

The factor *c* is one of the basic factors in the SMBE as defined in Figure 11. The outline of the total contributory area, A_{TL}, as carried by any one column, is identified by connecting the surrounding domes with straight lines through the HP centers. The total load on a column is calculated as:

$$\mathrm{W_{TL}} = \mathrm{qA_{TL}} \tag{14}$$

From this the required thrust H_2^F along the rim of the circular funnel is determined as:

$$\mathrm{H_2^F} = \frac{\mathrm{q(A_{TL} - \pi d^2)c}}{\mathrm{4\pi dh^{HP}}} \tag{15}$$

where *c* and *d* are defined in Figure 11. The ratio of these two thrust values, one along the rim of the circular funnel H_1^F and one along the top of the invert domes H_2^F, is given by the following expression:

$$RN = \frac{H_2^F}{H_1^F} = \frac{(A_{TL} - \pi d^2)}{2c\pi d(w_1^{HP/W} + 1)} \tag{16}$$

where H_1^F is the thrust along the common border with the (HP) and H_2^F is the radial thrust at the funnel rim. The value of *RN* is always found to be larger than one, and can be calculated for any structural membrane layout.

If the horizontal thrust for circular funnels is specified to be a constant, the corresponding differential equation for the funnel shape becomes:

$$\frac{\mathrm{dz}}{\mathrm{dx}} = \frac{\mathrm{(A_{TL} - \pi x^2)q}}{\mathrm{2\pi x H^F}} \tag{17}$$

for which the solution is:

$$z = A\ln(x/d) - B(x^2 - d^2) \tag{18}$$

with

$$A = A_{TL}w/2\pi H^F \; and..B = q/4H^F \tag{19}$$

With the above equations the SM variable heights *e* and the horizontal thrusts *H* in all units are determined.

In all SM shells, the total required thrust is calculated along the previously identified thrust lines. The forces acting along these lines is the sum of the unit thrusts in the shell, starting at the center of one dome on one side and proceeding to the center of the dome on the other side of the same thrust line. Using the shell/plate analogy, it is now possible to convert back to the plate bending moments by using the equation: $M = He$. With the thrust *H* known throughout the shell and knowing that *e* is the height of shell, the bending moments, *M*, can be calculated for the entire plate. With the three fundamental shapes of the SMA model known, the moment *M* is known throughout. Once the solution regions

are identified and with the four fall-line parameters used to describe each field, the overall solution in the form of positive and negative moments is obtained. At this point it is convenient to borrow the terms "column-strip" and "middle-strip" from flat plate designs (Figure 6). In this effort the column-strip and the middle-strip moments are independently analyzed. To establish form continuity, these initial moment-areas are summed up and made equal to zero by the addition of two uniform moments ΔM_{ms} and ΔM_{cs} respectively. These are given by the equations 20 and 21 for the middle strip and the column strip, respectively.

$$\Delta M_{ms} = -\frac{2}{3}\frac{(M_1^D a + M_1^{HP} b)}{(a+b)} \tag{20}$$

$$\Delta \mathrm{M}_{CS} = -\frac{\frac{2}{3}(M_2^{HP} c) + M_{avg}^{1-1} R\, c}{c+d} - \frac{(\frac{1}{6} M_{avg}^{1-1} + \frac{2}{3} M_{avg}^{2-2})(d - R_c)}{c+d} \tag{21}$$

The results represent the fixed-end-moments for the slab subjected to the given loading. Saether (1994)

2-D Moment Distribution

For 2-D rigid frames, with fixed-end-moments determined for any particular layout, final moments may be determined by a 2-D moment distribution. This is a simple concept developed by Hardy Cross (1949). For a 3-D structure, such as the ones developed in the SMA, a 3-D surface oriented moment distribution has been developed. This is shown in the following. Before doing so it is necessary to recap some of the basic steps used in 2-D moment distributions.

For these frames the moment distribution consists of three steps. The first step calculates the fixed-end-moments for any giving loading and frame geometry. This establishes the moments as statically determined units assuming all supports to be fixed. The second step is to release the fixity at each column, one column at a time. As this takes place, the juncture between each column and the attached beams will undergo a rotation corresponding to the amount of unbalanced moments resulting from the initial fixed-end condition. Free to rotate, the unbalanced moment is brought into equilibrium by small moments developing in the connected components at this juncture. The sum of these will match the unbalanced moments and establish equilibrium at the slab juncture, now assumed fixed in its new position.

The rotation of a member at any one juncture will cause small moments to be generated at the far ends of these members, which remain fixed at this stage. These carry-over moments are calculated for each juncture as a third step. This results in a series of new

unbalanced fixed-end-moments, located in the slabs at the column supports. A second iteration is necessary using the same three steps. First the newly established fixed-end-moments are summed up, these are balanced and the effects of these balanced moments are subsequently carried over to the adjacent supports.

In these efforts it is important that each corrective step is calculated before the next sequence is started. Because several components are feeding part-moments into any slab juncture, these components must be stored in a separate, temporary file, and only distributed after the previous sequence has been completed for all supports. Only after these part-moments have been balanced and distributed can the first batch of distributed balancing moments be allowed to merge into the originally determined fixed-end-moments. In this way the correct amount of balancing is assured at each completed iteration.

Only after each step has been carried to its completion at every juncture the next sequence may be contemplated. Diagram A illustrates the iteration procedure.

Moment Distribution in Flat Plates

The surface oriented 3-D moment distribution in flat plates follows the same three steps as outlined above. Certain modifications are required, however. The first step of establishing the unbalanced moment is done by a vectorial addition of the fixed-end-moments (Figure 14). This determines the magnitude of the unbalanced moment M_{unbal} and its direction α. The second step is to create equilibrium by relaxing the fixity at each support and allowing their moments to be balanced by small moment corrections in all connected components. (Figure 15). This may be referred to as a surface oriented moment balancing. The third step is to calculate the magnitude of any carry-over moments caused by this balancing, making full allowance for the relative column and slab stiffness of each component while assuming that all adjacent supports are fixed. These corrections add unbalanced moments at these adjoining column supports.

These new unbalanced moments, however, must be balanced in a second iteration. In this way, after a series of iterations, these corrections to the negative column and middle-strip moments make up the final slab moments. Corresponding adjustments in the column reactions and in the positive column-strip and the positive and negative middle-strip moments complete the analysis. The number of iterations is selected so as to ensure convergence within a pre-selected tolerance dependent on the selected convergent tolerance.

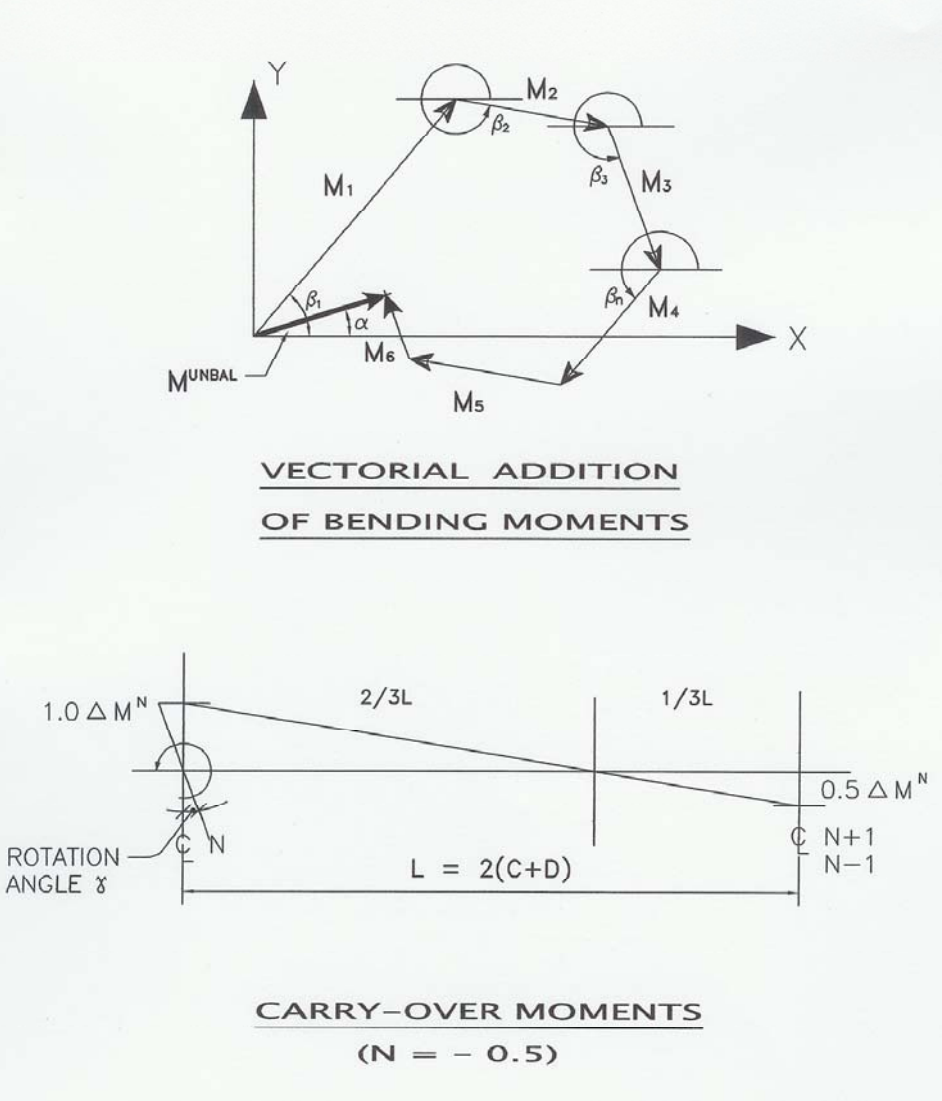

Figure 14. Basis for moment distribution.

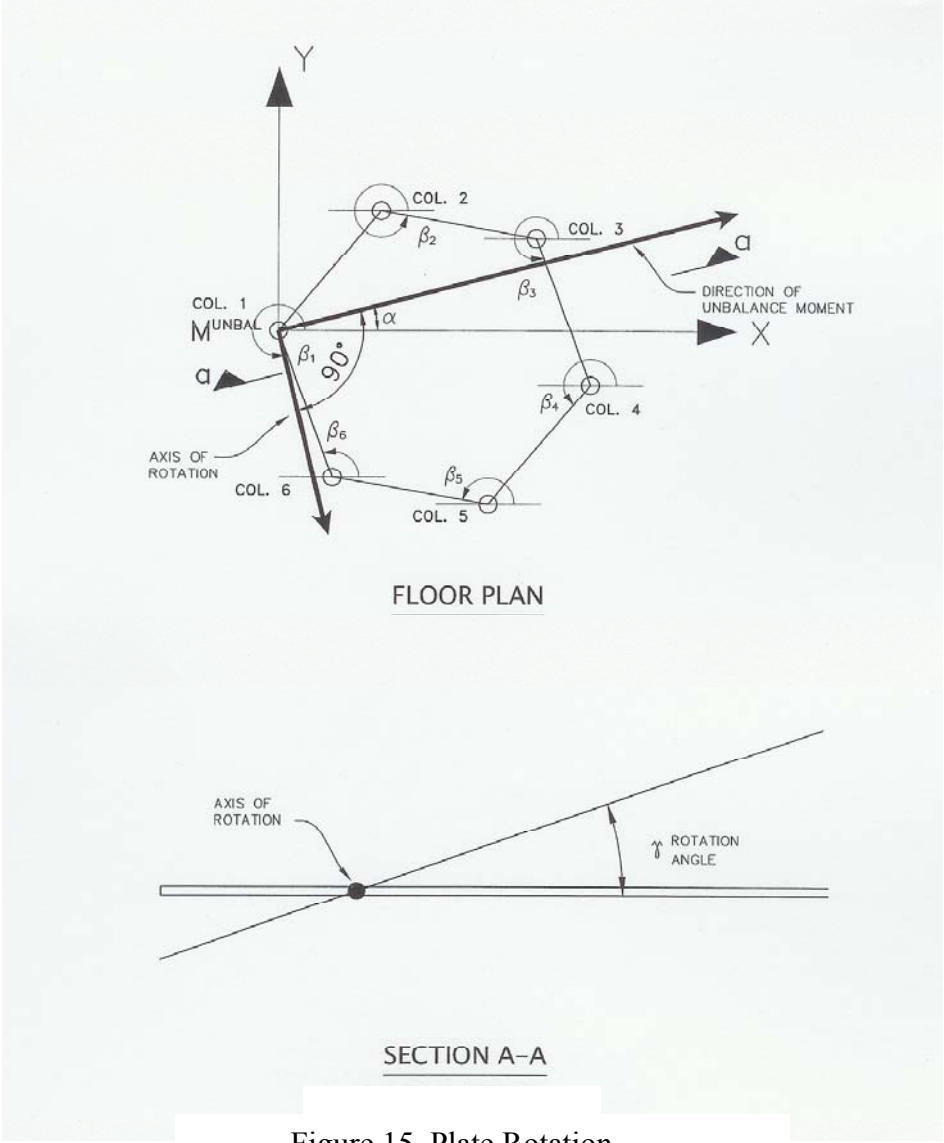

Figure 15. Plate Rotation

Assumptions

In the moment balancing efforts there is no need for solving problems with a multitude of unknowns. The unbalanced moments are evaluated and distributed to the various components corresponding to their relative stiffness. A number of assumptions are made,

however. To arrive in the original SMA analysis at the two delta-moments needed in the fixed-end-moment calculations for balancing the positive and negative moments in the slab, prismatic cross sections of the slab components were assumed. The same is assumed in calculating the carry-over moments in step three. During the structural membrane calculations it was assumed that the uniform load would be distributed 50-50 in two orthogonal support directions. These assumptions furnish results that are easily obtained and are found to deliver good approximations to the true answer.

The initial assumption of an equally divided load in the orthogonal directions is accurate for square, equal-lateral triangular and hexagonal layouts. The prismatic profile for the various slab components is fairly accurate for any rectangular layout and is assumed to be a valid approximation for most irregular layouts. A further justification for these assumptions in calculating the carry-over factor is that they only affect the corrective moment components with relatively small effect on the overall results.

The interaction between a flat plate and the supporting columns is complicated and has been the subject of numerous studies Corley (1961). Because of the cracking that takes place next to the columns due to the peak moments at this location, an exact prediction of the relative stiffness can not be made. As the slab cracks and the reinforcing steel begins to yield, the slab stiffness and its resulting rotation undergo hard to predict changes.

It could be assumed that the stiffness of the entire width of the slab would participate, or that the stiffness of the column strip alone would be involved. It could include the balancing of the column and middle strip end moments separately or in combination. One possible assumption would be to balance all end moments, but use only the stiffness of the column strips in determining the relative stiffness of the slab.

For this paper it is judged to be sufficiently accurate to use the SMA factors *a* and *b* for the effective slab widths, and to use the ACI-318 equivalent column for the stiffness of the columns.

Details of the moment balancing and the surface oriented moment distribution are shown in the following. Initially, for all columns, the column moments from the initial fixed-end-moment calculations multiplied by their contributory widths, *a* and *b*, are added vectorially. The resulting unbalanced moment, M_{unbal}, acting in directions α as shown in Figure 14, are obtained. These M_{unbal} are distributed to the various slab components along the column lines and to the corresponding columns according to their relative stiffness:

$$k = K_n \Big/ \Sigma_1^m K_n \tag{22}$$

where K_n is the stiffness of the various slab components

$$K_{slab} = \frac{(a+b)t^3}{6(c+d)} \tag{23}$$

where *a*, *b*, *c* and *d* are the basic SMA parameters, and the stiffness of the column is:

$$K_{col} = \frac{Wd^3}{12h_c} \tag{24}$$

where h_c is the column height to the slab below or above the slab in question and where *d* and *W* are the length and width of the column, respectively. Rotated columns and circular columns are easily accommodated. In these calculations, where α is the direction of the unbalanced moment and β is the direction of the various resistive slab components, as given by the slab column lines, the latter forms the angle $(\beta - \alpha)$ with the unbalanced moment (Figure11). As the slab rotates by the amount γ_{max} in the direction of α, as caused by the unbalanced moment, the amount of rotation of each component within the slab amounts to the value γ reduced by the factor $\cos(\beta - \gamma)$. That is, the rotation of any of the connected members within the plate is $\gamma_{max} \cos(\beta - \alpha)$.

$$\Delta M^n_{act} = k_n M_{unibal} \cos(\beta - \alpha) \tag{25a}$$

Furthermore, the effective moment $M_{eff.}$ in resisting the M_{unbal} is the ΔM^n_{act} in each slab component reduced by a similar factor cos(β-α). This will allow for the fact that if the angle (β-α) = 0, the moment is in direct line with the unbalanced moment M_{unbal} and therefore is resisting this rotation with its full value. Similarly, if the angle $(\beta - \alpha) = 90^o$, the moment is normal to the rotation and, by ignoring any torsional resistance, would have no effect in resisting the unbalanced moment. This is shown in Figure15. As a result, the effective component of the moment, $\Delta M^n_{eff.}$ resisting the rotation is this moment $\Delta M^n_{act.}$ multiplied by the factor $\cos(\beta - \alpha)$, or in other words:

$$\Delta M^n_{eff.} = k_n M_{unbal.} \cos^2(\beta - \alpha) \tag{25b}$$

To obtain the desired accuracy, moment balancing will be subjected to a series of iterations. With a carry-over-factor of *n* = -0.5, which applies to prismatic beams, this iteration is carried out until the total sum of changes in moments, from the initial amount of adjustments, is below a given tolerance. (See diagram A)

After the moment distribution has been completed, the corrective moment in the direction of each span can now be calculated as:

$$\Delta M^n_{act.} = \frac{\Delta M^n_{eff.}}{\cos(\beta - \alpha)} \tag{26}$$

This moment is added to the initial unbalanced moment:

$$\Delta M^\eta_{act} = \Delta M^\eta_{init} + \Delta M^\eta_{act} \tag{27}$$

As moment balancing takes place, the column loads in the affected columns are corrected to correspond to the adjustments in the slab bending moments at these columns. This correction is:

$$\Delta P = \frac{\Delta M_{act.}}{2(c+d)} \tag{28}$$

The individual values of *c* and *d* are the original parameters obtained from the SMA analysis as shown in Figure 11.

The described approach delivers the final negative moments at the column supports. To be used in cases similar to where the ACI-318 Equivalent Frame Method is applied, these moments may be averaged. It must be remembered, however, that this averaging is only allowed where the resulting sections are under-reinforced.

Basically, the total resistive moment offered by any one strip radiating out from a column is the sum of the computed average negative unit moments multiplied by the corresponding slab widths *b*, plus the negative middle strip moments multiplied with the width *a* of the middle strip. Because these moments in an irregularly supported slab are acting along the randomly oriented column lines, it is desirable to obtain design moments that are acting along the selected *x* and *y* axes of the slabs. These moments may be obtained by vectorially adding these various balanced moments. This is explained in the following: At each column, the acting bending moments are multiplied with the appropriate values of $\cos\beta$ and $\sin\beta$ to establish the moment components in the *x* and *y* directions. Next, all values of $M\cos\beta$ larger than zero are added up to give the total M_x^+ and all values smaller than zero are added to give the total M^-_x. The same procedure is applied to the values of $M\sin\beta$. The sum of values larger than zero gives the total M_y^+ and the sum of values smaller than zero give the total M_y^-.

$$M^+_{x\,\mathrm{Final}} = \Sigma M\cos\beta \qquad \texttt{(for values of cos } \beta \texttt{ > 0)} \tag{29}$$

$$M^-_{x\,\mathrm{FINAL}} = \Sigma M\cos\beta \qquad \texttt{(for values of cos } \beta \texttt{ < 0)} \tag{30}$$

Similarly the final M_Y moments are established

$$M^+_{y\,FINAL} = \Sigma M\sin\beta \quad \texttt{(for values of sin } \beta \texttt{ > 0)} \tag{31}$$

$$M^-_{y\,FINAL} = \Sigma M\sin\beta \quad \texttt{(for values of sin } \beta \texttt{ < 0)} \tag{32}$$

In these sums the positive and negative column- and middle-strip moments have been multiplied by the corresponding values of *a* and *b*, respectively. Each sum so established is then divided by the sum of the corresponding *b* and *a* values, to arrive at the final average unite design moments. If these linear sums of *b* or *a* exceed the actual available column strip, respective middle strip widths, the sum should be limited to these available

widths, while the unit moments should be increased accordingly by the factor $b_{calculated} / b_{available.}$.

The results of the SMA have been compared to various existing design methods. This includes, among others, finite element calculations for irregular layouts as well as the ACI-318 equivalent Frame Method for the analysis of regular flat plates. Some of these comparisons have been shown in Saether (1994) and other comparisons are presented below. Figure 16 shows a typical irregular column layout that is used for comparison studies. Columns 6, 12, 13, and 14 have been identified as presenting a challenge in the prediction of strip moments M_{11} and M_{22} in the x and y coordinate directions, respectively. Figure 17 shows the output of moments using the finite element code ETABS. The contour plot shows large jumps in the moments predicted around the column. Aside from concerns over convergence of the solution, it is not possible to directly obtain average moments using ETABS. Detailed calculations were made to compare ETABS column strip moments M_{11} and M_{22} with SMA calculations. Figures 18 through 25 show the predictions of ETABS and SMA for the column strip moments M_{11} and M_{22} for selected columns. The SMA predictions show a close agreement with the finite element results.

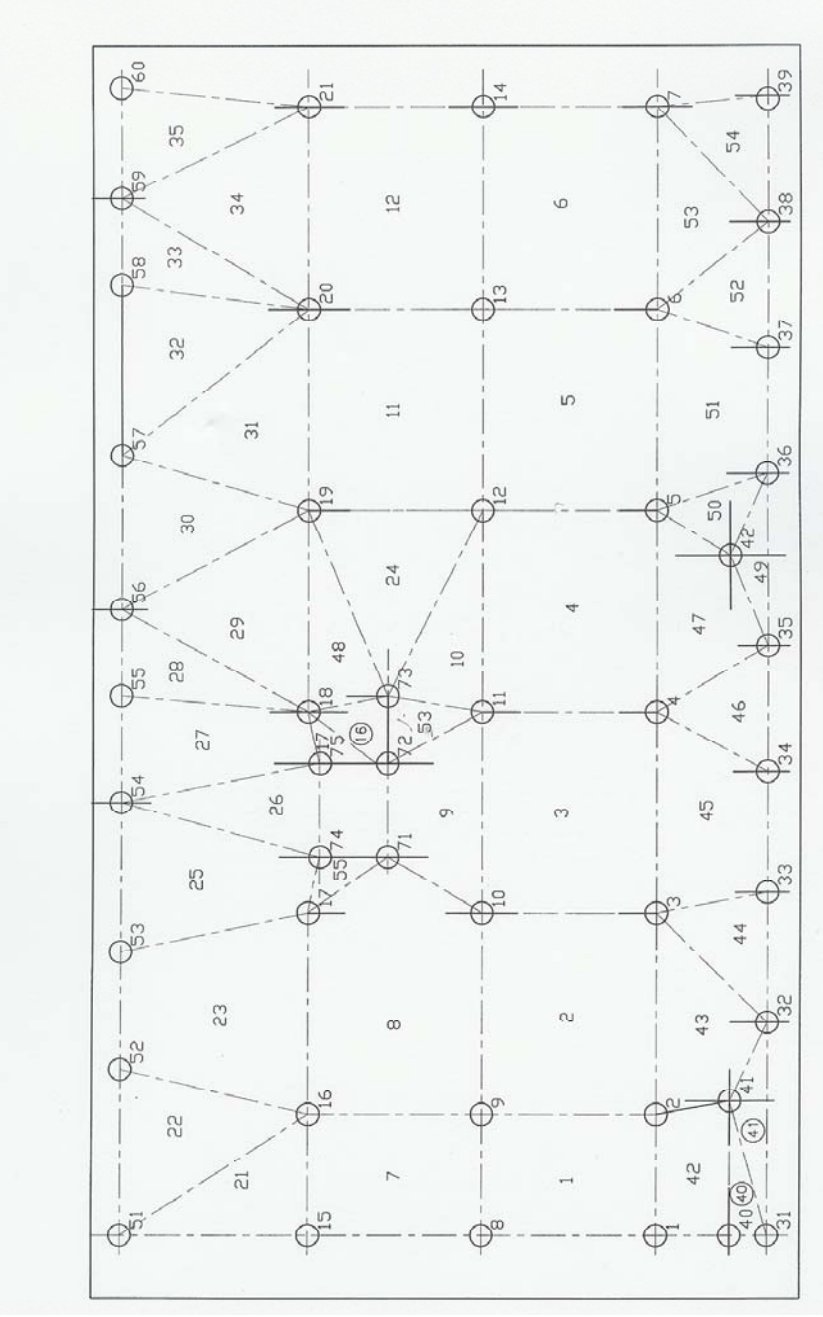

Figure 16. Typical floor plan with irregular column arrangement.

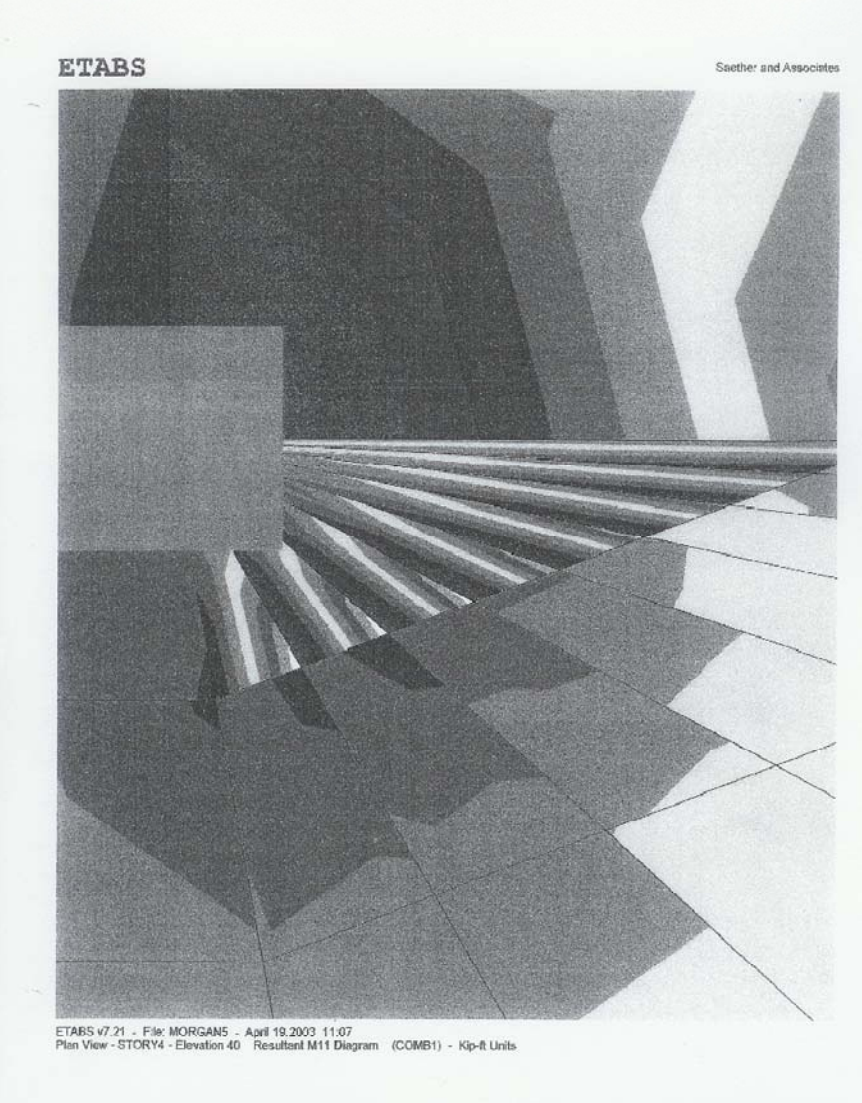

Figure 17. ETABS bending moments at one column in a triangular field.

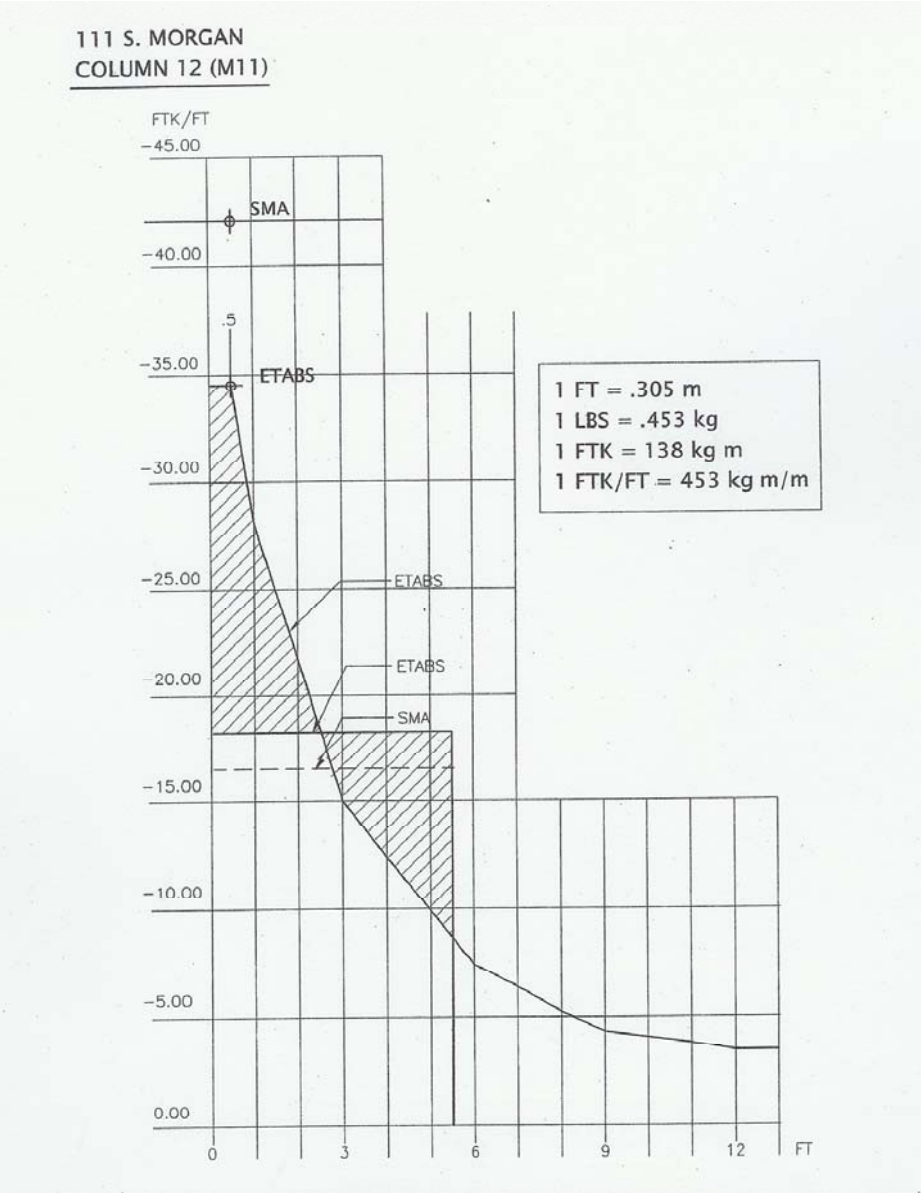

Figure 18. Maximum and average M_{11} moment comparisons between SMA and ETABS at the face of column number 12.

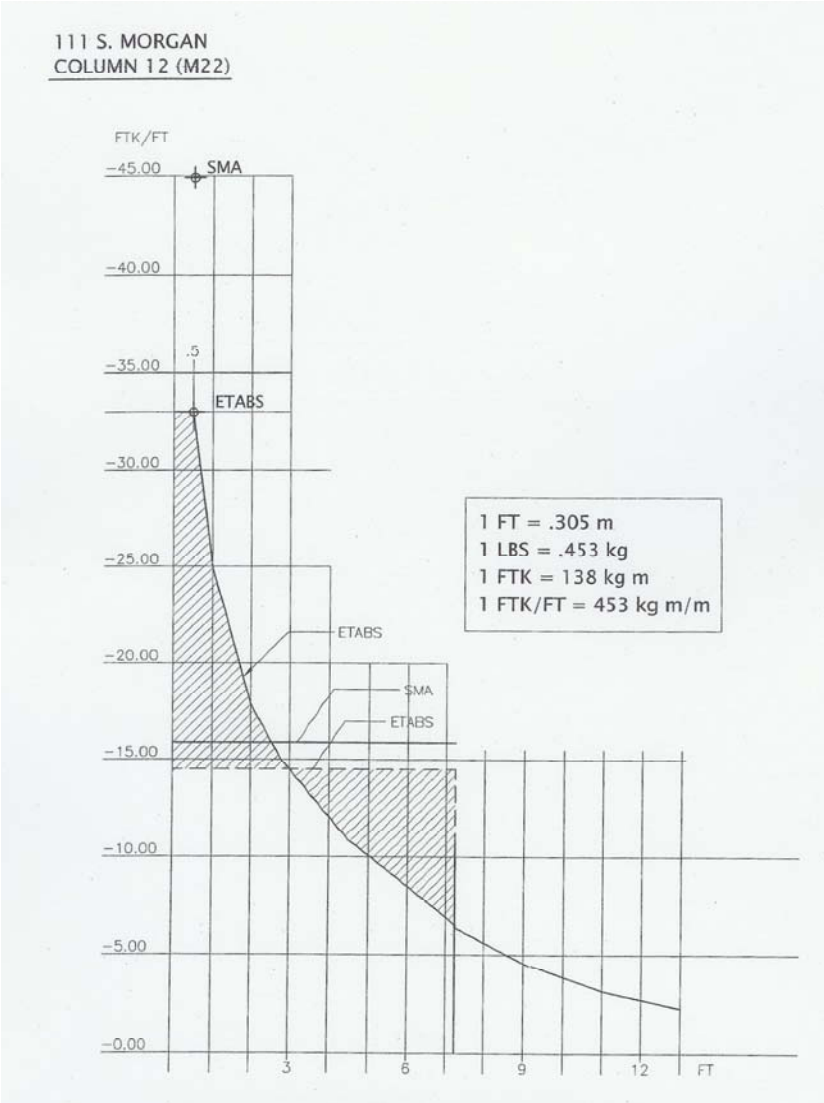

Figure 19. Maximum and average M_{22} moment comparisons between SMA and ETABS at the face of column number 12.

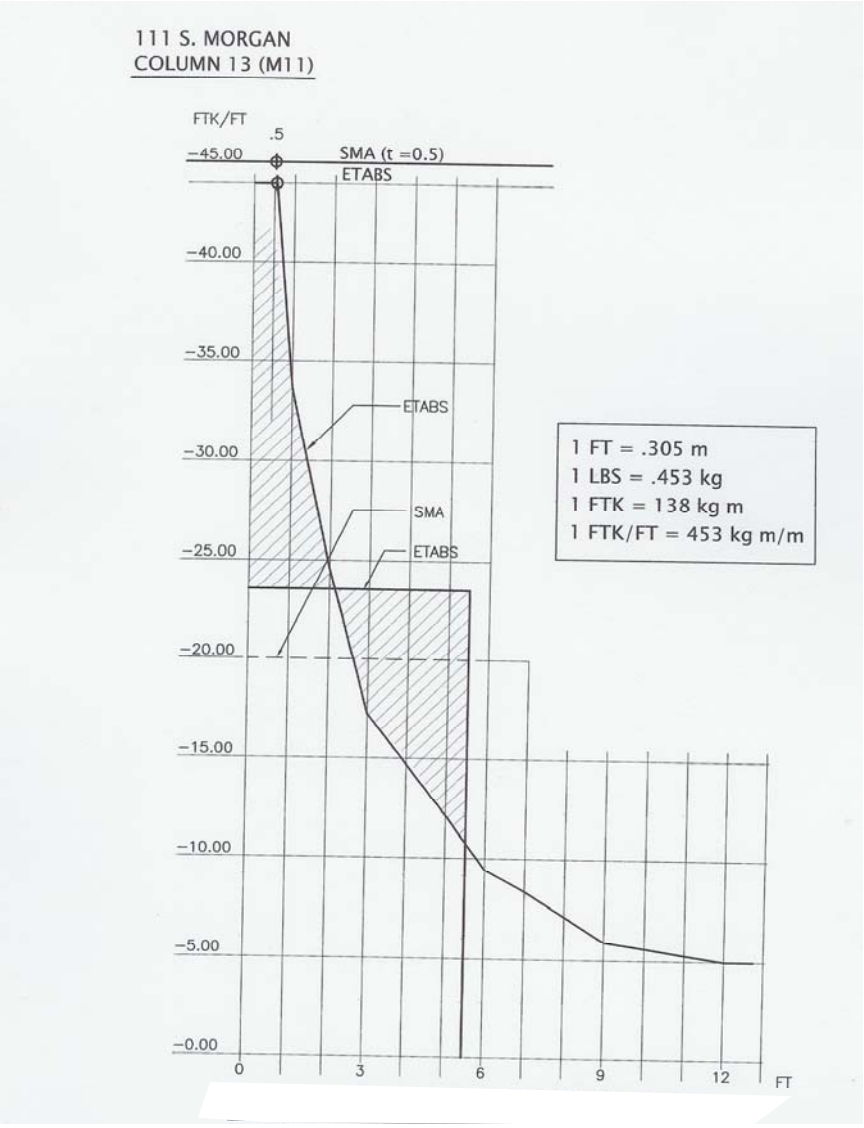

Figure 20. Maximum and average M_{11} moment comparisons between SMA and ETABS at the face of column number 13.

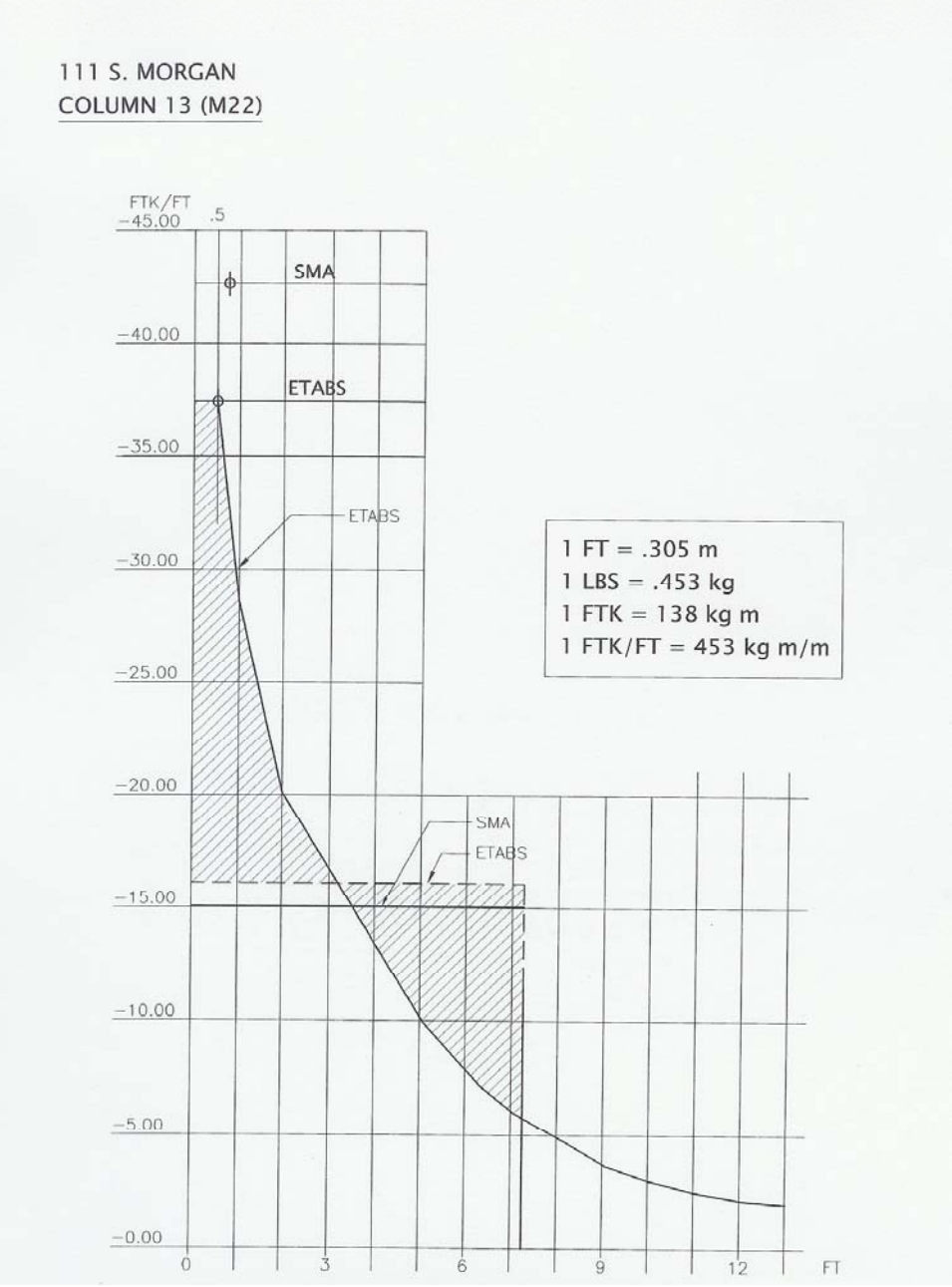

Figure 21. Maximum and average M_{22} moment comparisons between SMA and ETABS at the face of column number 13.

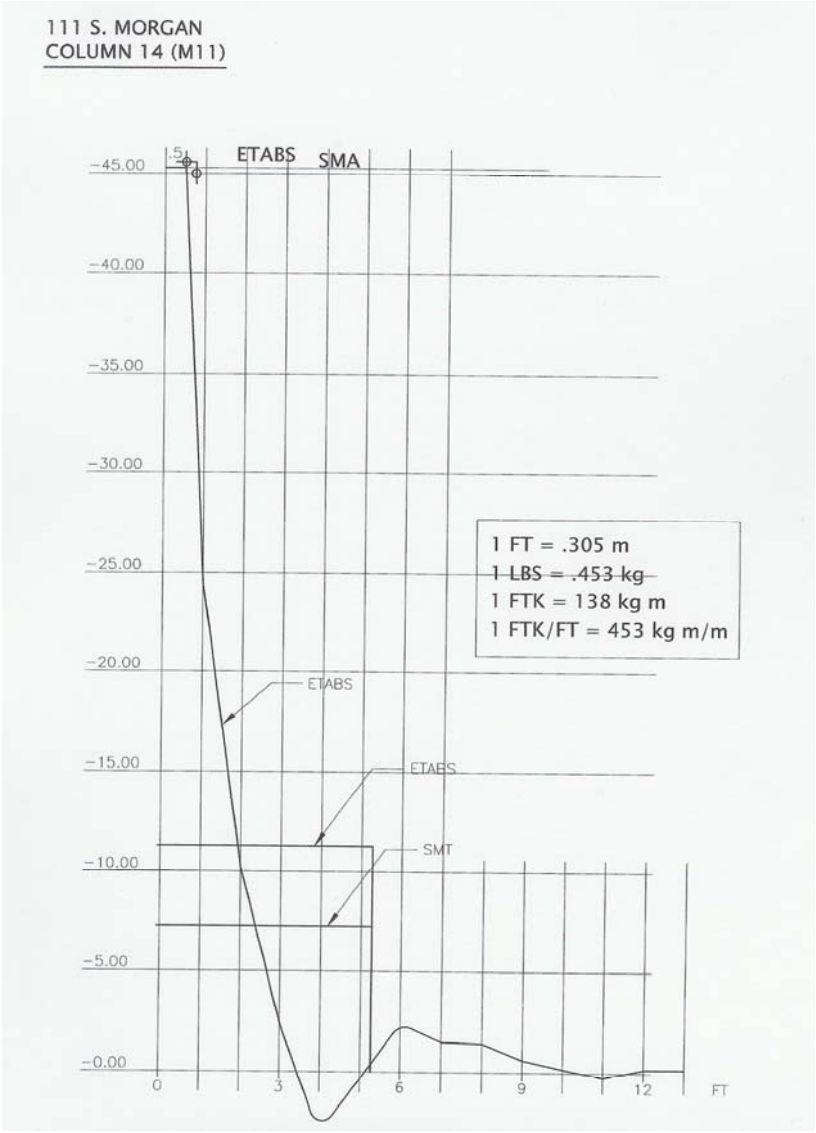

Figure 22. Maximum and average M_{11} moment comparisons between SMA and ETABS at the face of column number 14.

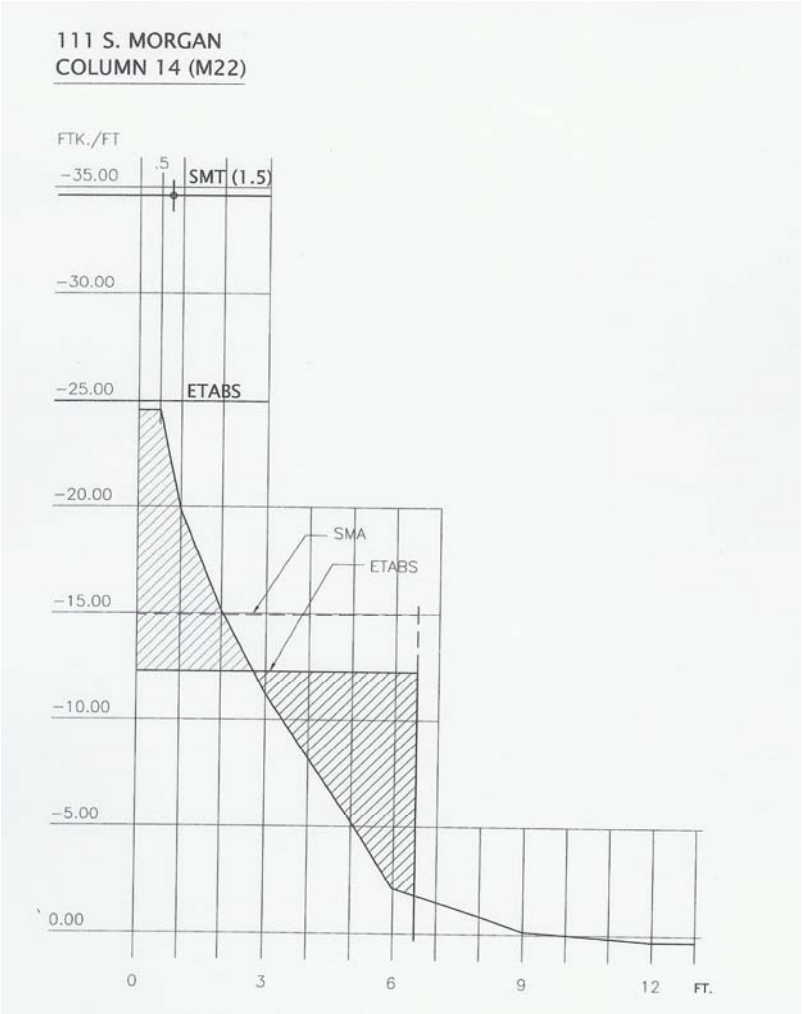

Figure 23. Maximum and average M_{22} moment comparisons between SMA and ETABS at the face of column number 14.

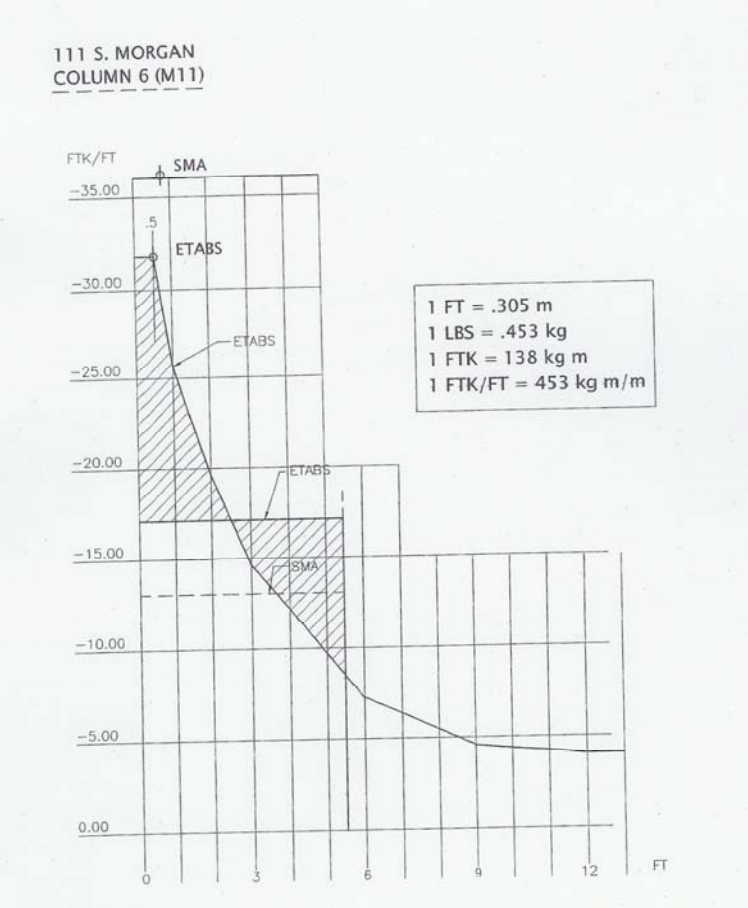

Figure 24. Maximum and average M_{11} moment comparisons between SMA and ETABS at the face of column number 6.

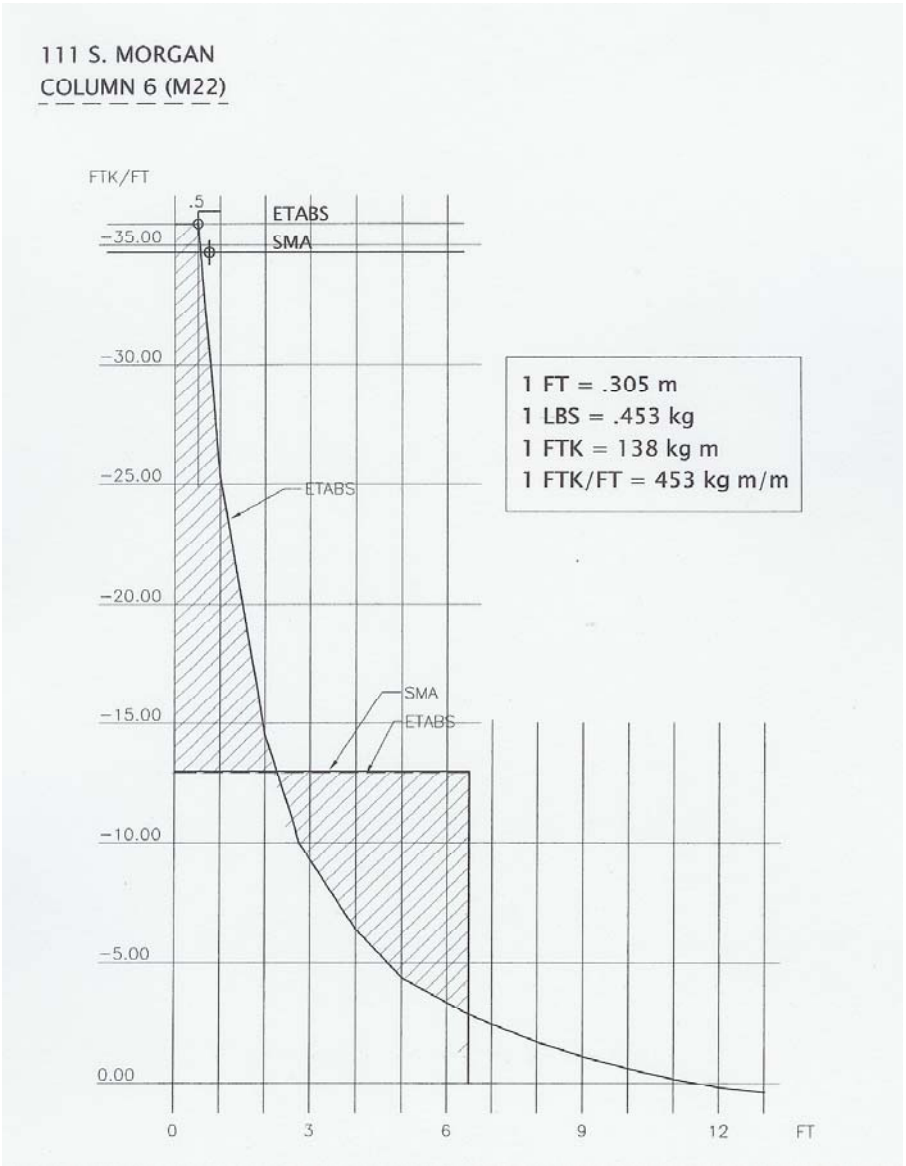

Figure 25. Maximum and average M_{22} moment comparisons between SMA and ETABS at the face of column number 6.

Diagram A.

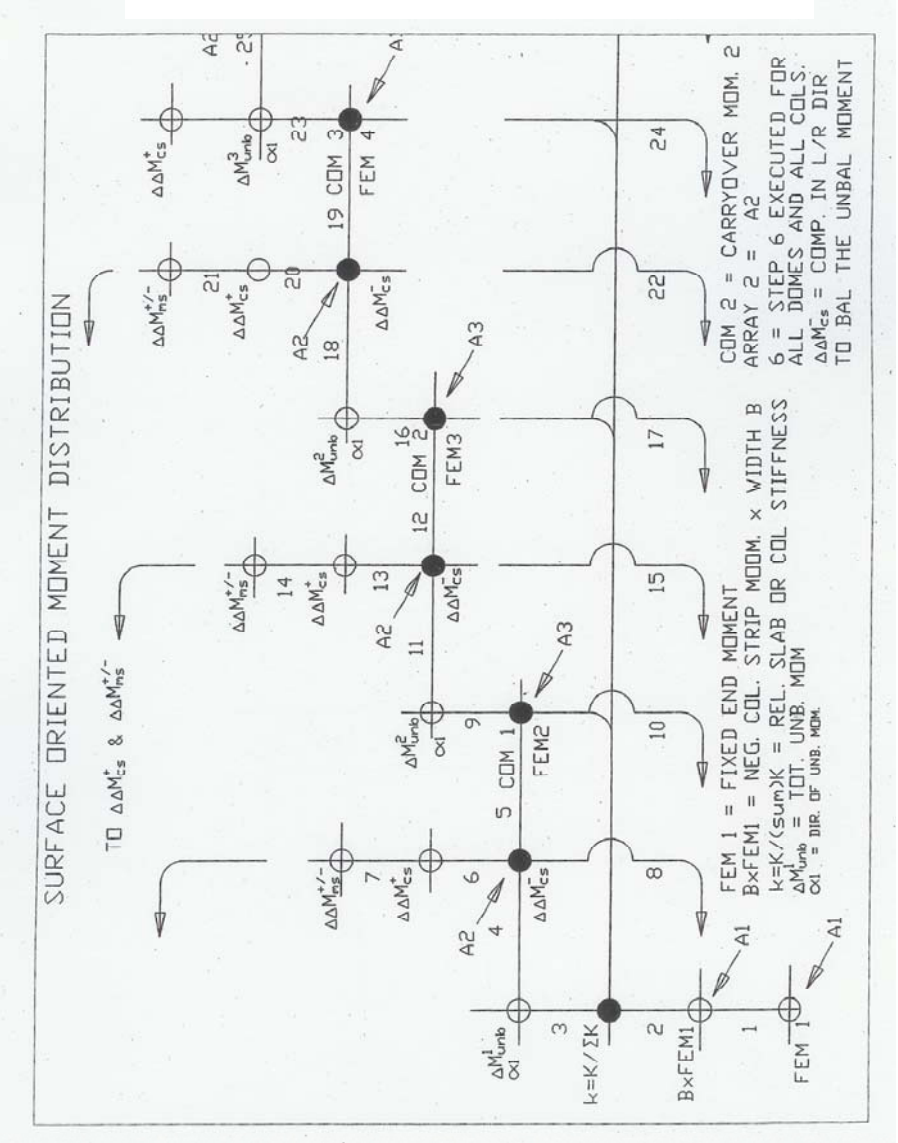

Summary

The basic SMA approach, as published in Saether (1994), has been expanded in this paper to include the determination of the governing column lines. Furthermore, surface oriented 3-D moment distribution has been added to arrive at final slabs design moments.

The following is a summing-up of the SMA:

1) It is one of few design models that will analyze an irregularly supported flat plate in one complete, quick and continuous analysis.
2) Comparisons have proven that it will deliver accurate final, adjusted maximum and averaged slab moments and adjusted column reactions.
3) It analyzes slabs with uniformly distributed loads.
4) The uniform load may vary from one field to the next. Checkerboard live load arrangement is possible.
5) Bi-axial column bending is part of the standard SMA output.
6) A computer program allows a simple input to be applied and even for large, irregular slab layouts the runtime is reduced to a matter of some few seconds.

Appendix, Notations

A = size of slab area
a = Fall line parameters in the SMT
b = Fall line parameters in the SMT
c = Fall line parameters in the SMT
d = Fall line parameters in the SMT
d = depth of column
E = Young's Modulus of elasticity
H = thrust in the shell
$h_1^D h^{HP}$ = dome or HP heights
h_c = height of column
I = moment of inertia
K = total stiffness
k = relative stiffness
l = span length
M = slab moment
M_x = moment in X – direction
M_y = moment in Y – direction
ΔM = change in moment
n = SMT parameter
P = concentrated load
ΔP = change in column load
q = uniformly load
t = slab thickness
w = uniform load
w = width of column
α = direction of slab rotation
β = direction of column line
γ = slab rotation

References

1. Timoschenko, S., and Woinowsky-Krieger, S. “Theory of plates and shells”. McGraw-Hill Book Co., New York, N.Y., 1959.
2. Saether, Kolbjorn “The Structural Membrane”. ACI Journal, 32 (7), 827-850, 1961.
3. Saether, Kolbjorn “Flat plates with regular and irregular column layouts I & II”. ASCE Journal, Vol. 120, (5), 1999.
4. Saether, Kolbjorn “Structural membrane shells”. *International Association for Shells and Special Structures.* International Symposium, Milan, Italia, 1995.
5. Park, Robert. ,Gamble, William L. “Reinforced concrete slabs”.*2nd edition*, New York: Wiley, 2000.
6. Hardy Cross “Analysis of Continuous Frames by Distributing Fixed-End-Moments”. L.B. Grinler. Ed. New York, 1949.
7. Corley, J. and Jirsa, J. “The equivalent frame analysis for reinforced concrete slabs.” Dept. of Civ. Engrg., University of Illinois, Urbana, Illinois, 1961.